Regulation of dendrite development via target derived retrograde signals in the *Drosophila* larva

Tomos O. Prŷs-Jones

St John's College

August 2014

This thesis is submitted for the degree of Master of Philosophy

Declaration

This thesis is the result of my own work and includes nothing which is the outcome of work done in collaboration.

This thesis does not exceed 20,000 words.

Acknowledgements

I am extremely grateful to both of my supervisors, Dr. Matthias Landgraf and Dr Maarten Zwart, for their continued support and advice throughout this project. I would also like to thank everyone from the basement of the Zoology Department. I feel privileged to have worked amongst such welcoming and inspiring people. I would finally like to thank St John's College for welcoming me back after a year away.

Summary

Retrograde signals are diffusible, secreted, or membrane bound factors that transmit information from the post- to presynaptic membranes of a synapse. They have long been recognised as important factors in determining the development of neural networks. On receiving a retrograde signal, a neuron's pre- and postsynaptic neurites can undergo morphological or physiological changes.

In this thesis I have used the accessible and well-characterised locomotor system of the *Drosophila* third instar larva to investigate retrograde signalling between the dorsal anterior 1 (DA1) muscle and anterior corner cell motoneurons (aCC MNs). Previous studies with *Drosophila* demonstrate that muscle-derived retrograde signals are involved in the growth and homeostasis of the neuromuscular junction. In this project I have focused on the central changes that occur in the dendritic arbor of the motoneuron.

For my experiments I bred a stock of flies that expressed Gal4 in the DA1 muscles and LexA in the aCC-MNs. Therefore using the *UAS-mCD8-GFP* and *LexAop-myr::cherry* reporters ensured that the muscles fluoresced green and the MNs red. This genotype allowed me to target the expression of genes to the DA1 muscles. In this way I could express transgenes that alter muscle size (*UAS-myrPi3K* and *UAS-Cyclin E*), and then observe the corresponding changes in the MN dendrites.

As a muscle grows its synaptic resistance decreases, meaning that a larger current is required to depolarise the cell. The hypothesis behind this project was that retrograde signals could induce a longer dendritic arbor when innervating a muscle that is hypertrophied (vice versa for smaller muscles). This is based on the fact that longer arbors receive more presynaptic stimulation from interneurons, and this results in longer bursts of action potentials along the MN axon. Therefore a longer arbor restores physiologically appropriate levels of muscle depolarisation in larger muscles.

The results of this thesis suggest that the size of the DA1 muscle determines the length of the contralateral arbor in the aCC motoneuron. This is a localised effect as the ipsilateral arbor does not appear to be affected.

This project therefore supports the hypothesis that muscle-derived retrograde signals can regulate the dendritic complexity of a motoneurons in third instar *Drosophila* larvae.

Table of Contents

Abbreviations and acronyms

aCC	anterior Corner Cell
AEL	After Egg Lay
CNS	Central Nervous System
DA	Dorsal Acute (muscle)
DO	Dorsal Oblique (muscle)
FLP	Flippase
FRT	Flippase Recognition Target
FTIR	Frustrated Total Internal Reflection
GFP	Green Fluorescent Protein
Gbb	Glass bottom boat
IR	Infra-Red
MN	MotoNeuron
mRFP	monomeric Red Fluorescent Protein
myr	myristoylated
NGF	Nerve Growth Factor
NMJ	NeuroMuscular Junction
PNS	Peripheral Nervous System
RFP	Red Fluorescent Protein
RP2	“Raw Prawn” 2 (motoneuron)
SCG	Superior Cervical Ganglion
UAS	Upstream Activating Sequence

VNC	Ventral Nerve Cord
Wit	Wishful thinking

1 Introduction

The primary role of neurons is to receive, integrate and transmit information in the form of an electrical signal. Neurons have a highly polarised morphology with two main types of dendritic processes that project form the soma: a highly branched dendritic arbor that collects synaptic inputs and a smooth axon that terminates with a synapse onto a target cell. This asymmetric morphology might suggest that neuronal signalling is unidirectional, however communication is in both directions, and retrograde signals play an important role in the development of neural networks.

Studies have shown that retrograde signalling influences both dendritic and synaptic morphology. By crushing or ablating the axons of the mammalian superior cervical ganglion neurons researchers have observed a retraction in dendritic processes[1–3]. Only upon the recovery of the axon and re-innervation of the target cell do the dendrites re-extend to an otherwise unperturbed length. Research in the fly motor system has primarily focused on the effects of retrograde signalling at the neuromuscular junction (NMJ), with little attention paid to their effect on dendritic development[4–12]. This project investigates the influence of retrograde signalling on dendritic complexity of *Drosophila* larval motoneurons (MNs). Only by considering the bidirectional communication between neurons can we fully comprehend the development and output of neural networks[13].

In the following paragraphs I introduce *Drosophila* as the model organism, the fly motor system, early dendritic development, and factors that influence dendritic growth. I conclude the introduction with the specific question addressed in this thesis.

1.1 *Drosophila* as a model organism

The genetic amenability, size and generation time of *Drosophila* melanotgaster makes it an excellent model organism[14–19]. The *Drosophila* larva also has the advantage of being relatively simple with regards to musculature, motoneurons, and behavioural repertoire. The locomotor system is well characterised and it has been the subject of many studies in neuronal development.

The cylindrical body plan of the *Drosophila* larva can be subdivided along the anterior-posterior axis into a head, three thoracic, and eleven abdominal segments[20]. A cuticular exoskeleton surrounds the larva onto which the internal and external muscles are attached[16,21]. Hook-shaped structures (denticles) protrude from the exoskeleton giving the larva a grip on the external substrate. The two sets of locomotor muscles lie in the periphery of the body cylinder: the internal muscles span each segment along the anterior-posterior axis of the animal and at a perpendicular orientation, along the dorso-ventral (or transverse) axis, lie the external muscles. The muscles and body fluids act as a hydrostatic skeleton during locomotion[22]. Larval crawling is a peristaltic wave of contraction that starts in the posterior tip of the animal and progresses anteriorly[23,24]. In each segment the external muscles contract first causing the segment to circumferentially constrict and extend along its anterior-posterior axis. Contraction of the internal muscles then shortens the segment, pulling the denticles across the surface, and allowing them to attach in a new location. As the wave of excitation reaches the anterior tip of the animal, the anchoring mouth hooks release the substrate and are pushed forwards by the resultant hydrostatic pressure.

Provided the surface is flat, such as a sheet of agar, larval peristalsis is rhythmic and stereotypical. The wave of muscular contraction travels seamlessly along the body in approximately one second. As soon as one cycle of contraction finishes in the head a new wave is almost immediately initiated in the posterior of the larva, as shown by electrophysiological recordings from the motoneurons[22,25].

Within each hemi-segment there is a highly stereotyped pattern of 30 muscles innervated by roughly 36 glutaminergic motoneruons[16,21,26,27]. Motoneuron cell bodies are located in the cortex of the ventral nerve chord (VCN) and the dendritic arbors project into the dorsal neuropil, where they synapse with ascending and descending cholinergic, GABAergic and glutaminergic interneurons[28–30]. A subset of these interneurons are elements in the larvae's central pattern generator (CPG), the neural network involved with coordinating peristaltic locomotion[31–33].

Axons leave the VCN via one of three nerve roots per hemisegment: the intersegmental, segmental and transverse nerves[27]. During embryonic development the choice of

peripheral branch through which the axons project is key to bringing the motoneurons to their appropriate and stereotyped target muscles[22,34]. Contact between motoneuron and muscle is made via the neuromuscular junction, a membranous and highly specialised pre- and postsynaptic structure in which the synapses are located[35]. Presynaptically the NMJ consists of a series of spherical structures called boutons, which resemble beads on a string, and contain multiple vesicle release sites (otherwise known as active zones).

From hatching to pupation the larva grows a huge amount[36]. The short developmental time and the large increase in size make the *Drosophila* larva a model system in the study of synaptic development and plasticity. Decreased synaptic resistance to larger muscles necessitates an increased input current into the muscle to maintain physiologically appropriate levels of muscle depolarisation. Because there is no motoneuron-neurogenesis during larval life, a larger current is achieved through growth and maturation of the NMJ[15,37,38]. The presynaptic membrane adapts through addition and growth of boutons, such that each bouton contains more glutamate-release sites (active zones)[38], and there is a concurrent increase in the number of glutamate receptor densities in the postsynaptic membrane.

The coordinated differentiation and growth of the larval NMJ is achieved, at least in part, from *Wnt* signalling (Fig 1). This family of small glycoproteins activates anterograde and retrograde signalling pathways, in the post- and presynaptic membranes respectively[39–42]. *Wingless* (wg) is a member of the *Wnt* family and is released into the synaptic cleft following presynaptic neuronal activity. Due to its hydrophobic nature it traverses the synaptic cleft in extracellular vesicles[43]. Larvae with mutations in the wg signalling pathway possess a large proportion of boutons in an early, undifferentiated state. These 'ghost-boutons' lack active zones, sub-synaptic reticulum, and have defects in their presynaptic microtubule cytoskeleton. Glutamate receptors also fail to form high density clusters due to disrupted scaffold proteins, namely *Discs Large*.

Postsynaptically, *Wingless* activates the novel F*rizzled* Nuclear Import (FNI) pathway by binding to the *Lrp5/6-dFrizzled-2* receptor complex[44]. The ligand-bound receptors are then endocytosed to a paranuclear location, where the *dFrizzled-2* carboxy-termini are cleaved and entre the nucleus. These associate with large ribo-nuclear protein particles

bearing synaptic protein transcripts that are directed back to the postsynaptic membrane to be locally translated[39]. The *Lrp5/6-dFrizzled-2* complex is also found in the presynaptic membrane, however activates a divergent canonical *Wnt* signalling pathway that influences cytoskeletal dynamics via the microtubule associated protein (MAP) *Futsch*[45].

Although *wg* has received the most attention to date, other *Wnt* signals are believed to act synergistically to coordinate the development and plasticity of the Drosophila NMJ. *Wnt-5* positively regulates NMJ development, at least in part through the *Derailed* receptor[46], whereas *Wnt-2* acts as a retrograde negative regulator of presynaptic growth. Larva mutant for *Wnt-2* have increased branching at the NMJ.

Evenness Interrupted (*Evi*) is an important transmembrane protein involved in the secretion of *wg*, its journey across the synaptic cleft, and the targeting of the Lrp5/6-dFrizzled-2 complex to the postsynaptic nuclei[43]. The membrane permeability of *wg* facilitates its binding to *Evi*, and requires that the *wg-Evi* complex is transported around the motoneuron in vesicles. Goodman et al (2006) showed that *Evi* is involved with bidirectional trafficking of *wg* between Golgi apparatus and plasma membrane, with mutants exhibiting a somatic accumulation of *wg*[43,47]. At the postsynaptic membrane, *Evi* is necessary for the association between the internalised *dFrizzled-2* receptors and *GRIP*, a protein that directs vesicles towards the sub-synaptic nuclei.

Only recently have researchers turned their attention to changes that occur in the central nervous system during larval growth[36]. In this project I am looking at the central changes that occur when a motoneuron innervates a target muscle that is bigger or smaller than normal.

1.2 Early dendritic development

Like many neurons, dendritic development in the *Drosophila* larval motor system is preceded by the establishment of a nascent axon[48,49]. Dendritic processes are first observed extending from a region of axon called the primary neurite during embryonic development, approximately 12 hours after egg laying (AEL). Previously dendogenesis was believed to be a rather passive process. However with the development of

membrane bound GFP, live imaging has revealed that the early dendritic arbor is a highly dynamic structure with extension and retraction of multiple filopodia[49–54]. Only a subset of these filopodia are eventually stabilised.

In vivo live imaging of the developing zebrafish suggests that filopodial stabilisation is a result of active synapse formation[55]. By measuring the distribution of a fluorescently tagged postsynaptic marker protein (PSD-95), the authors were able to show that the majority of nascent synapses form on newly extended filopodia. The filopodia often over-extended before retracting back to a newly formed synapse. The majority of nascent synapses were not maintained, however stable synapses resulted in a filopodium becoming a stabilised dendritic branch. The authors assumed stable synapses to be active. This supports a synaptotropic model of dendrite formation, whereby the establishment of active synapses can direct the development of the dendritic arbor. However there is some debate as to whether synaptic transmission is necessary. In cultured hippocampal neurons the presence, and not activity, of the presynaptic neurons is sufficient for correct dendritic organisation[56]. Over the course of development the rate of extension and retraction decreases.

Whether stabilisation of dendritic branches is coordinated by synaptic transmission or simply contact, calcium appears to play a crucial role in the process. Both naturally occurring and induced waves of calcium influx into the arbor correlate with the stabilisation of nascent dendrites[57–59].

A filopodium undergoes a series of molecular changes as it becomes a stabilised dendritic branch[60]. There is a shift in cytoskeletal composition of the filopodia, from highly dynamic actin filaments to more stable microtubules[61]. While both types of neurites are stabilised by microtubules the orientation of these cytoskeletal elements is very different between axons and dendrites[62]. This is particularly obvious in *Drosophila* and suggests that a very simple model could explain neuronal polarisation. Microtubule subunits are polarised, with a minus and a plus end. In axons the majority of microtubules are plus-end-distally orientated while the dendrites are mainly minus-end-distally orientated [60]. This suggests that the segregation of organelles, synaptic components, protein synthesis machinery and other cytoskeletal proteins could be determined by their association with different

classes of motor proteins. Studies have generally focused on regulating the dynein or kinesin motor proteins. Dyneins are minus end directed and are heavily involved in ferrying dendrite-bound cargo, while kinesins move in the opposite direction. Mutating the dynein heavy chain disrupts organelle trafficking and results in the accumulation of mitochondria and golgi outposts at the cell body. The consequence of such a mutation is a shorter total dendritic arbor[63], however the local accumulation of golgi outposts in the soma results in a higher rate of proximal dendritic growth. Mitochondria that are normally distributed throughout the neuron are not observed in the dendrites when dynein expression is down-regulated[64]. Conversely mutating the plus-end directed kinesin-1 prevents mitochondria from entering the axon. So far most of the evidence has supported this simple model of neuron polarisation, although more work is needed to investigate whether the model fits monopolar neurons[62]. These are neurons, such as the *Drosophila* RP2 motoneuron, in which only one neurite extends from the soma.

The final shape and size of the dendritic arbor determines the processing and integration of electrical signals as well as the number of synaptic inputs it receives. The extreme variety of neuronal function is therefore mirrored by a large diversity of dendritic morphologies. The final shape of these dendritic arbors is determined by a balance between reducing metabolically active neural tissue and the need to cover the receptive field. Dendrites must occupy a volume of space where the appropriate presynaptic cells are located, make synapses with this subset of neurons, and adjust flexibly in response to experience.

The following paragraphs will discuss factors that influence the growth of dendritic arbors: retrograde signalling, the internal transcriptional programme, external cues, and activity.

1.3 Retrograde Signalling

The focus of this project will be the pronounced and well documented effect of retrograde signalling on neuronal morphology. A retrograde signal is generally a postsynaptic molecule that is either diffusible, secreted or in physical contact with the presynaptic cell. Many molecules have been established as retrograde signals, and have

been shown to act at various stages throughout development[65,66]. Since the discovery of neurotrophins[67,68], bone morphogenetic proteins (BMPs)[7,11,69], Wnts[25,70], endostatin[71], nitric oxide[72], endocannabinoids, and adhesion molecules[73,74] have been established as retrograde signals. Unlike anterograde neurotransmission, the effects of retrograde signalling are generally long lasting.

Due to its accessibility, the mammalian superior cervical ganglion has served as a model system in studying how the dendritic morphology of a neuron is affected by its connectivity with a postsynaptic cell[3,75]. The superior cervical ganglion normally grows in proportion with animal (rat) body size, however Voyvodic (1989) showed that cutting the submandibular salivary duct, and thus the ganglion cell axons, led to a smaller and simpler dendritic arbors with fewer input synapses. In contrast, by half cutting the submandibular salivary duct and partially denervating the salivary gland, the relative target size of the intact ganglionic cell was increased. This resulted in the remaining ganglion cells developing a more complex arbor with a greater number of presynaptic inputs. Presynaptic activity to the superior cervical ganglion was prevented during these experiments demonstrating that dendritic complexity was influenced by relative target tissue size.

Further evidence that connectivity with the target is important in determining dendritic complexity comes from axons that are severed and then allowed to re-innervate their target tissue[2]. There is a marked retraction in the arbor of ganglion cells two weeks after axotomy, however on re-innervating the target the dendritic arbor recovers to the size of an un-operated cell[76]. While this effect could be due to nerve damage, metabolic data suggest that this is improbable[77–79]. A more likely cause would be loss of some trophic signal[3,80].

Most studies have shown that axotomy leads to dendritic retraction, although this is not always true. Motoneurons innervating the neck muscles of the cat respond to axotomy by a dendritic expansion[81], and even within one organism distinct classes of motoneurons may respond differently to axotomy[82].

Research on signalling in the fly motor system has focused mainly on the NMJ. By blocking glutamate receptors in the postsynaptic membrane of the NMJ and reducing

muscle depolarisation below a physiologically appropriate level, researchers have shown that a target-derived signal acts homeostatically to increase the quantity of neurotransmitter released into the synaptic cleft[83–85]. Likewise the maturation of the mouse NMJ, with the incorporation of high-affinity choline transporters (CHTs), relies on activity dependant retrograde signalling[86].

Bone morphogenetic proteins (BMPs) are well documented retrograde signals in coordinating NMJ and muscle growth[9,87,88]. During the development of a *Drosophila* larva there is a 100-fold increase in muscle surface area[36] necessitating a concomitant growth of the NMJ to maintain physiological levels of muscle depolarisation. Over the course of larval development the NMJ responds with a 10-fold increase in bouton number as well as a 10-fold increase in the number of active zones per bouton[7,38]. Many studies have identified the ligand *glass bottom boat* (*gbb*) and its presynaptic receptor, *wishful thinking* (*wit*), as an important retrograde signal in directing this process (Fig 1)[7–9]. Compared to wild type larvae *Wit* mutants exhibit smaller synapses, severe defects in evoked junction potentials, a lower rate of spontaneous vesicle release and changes in the active zone structure.

The type II *wit* receptor forms part of a larger hetromeric receptor complex with a type I receptor, either *Thickvein* (*Tkv*) or *Saxophone* (*Sax*)[9]. Upon binding the *gbb*, the activated receptor complexes are endocytosed and the signal reaches the nucleus by dynein mediated retrograde transport. *Wit* phosphorylates the type I receptor, which in turn phosphorylates the cytoplasmic transcription factor *Mothers against decapentaplegic* (*Mad*). By binding to *Medea*, *p-Mad* can enter the nucleus and regulate gene transcription in the presence of nuclear co-factors.

The presynaptic cytoskeletal changes associated with BMP signalling are believed to be mediated by the *Rho* family of small GTPases[11]. *Rac* in particular is involved with the coordination of axon growth, branching and dendritic growth. The BMP signalling cascade regulates the expression of a *Rac*-activating guanine exchange factor (*Rac GEF*) called *Trio*. Thus it is easy to imagine that, as well as the NMJ, other aspects of motoneuron morphology are influenced by retrograde signalling.

Evidence suggests that BMPs act as a common signalling pathway involved in synaptic strengthening. Baines (2004) demonstrated that central synapses in the larval motor system are strengthened when *gbb* is expressed presynaptically. Additionally, many human pathologies such as hereditary spastic paraplegia exhibit defects in the BMP signalling pathways, suggesting that they are conserved across phyla[10].

So far little attention has been paid to the effect of muscle-derived retrograde signalling on the dendritic complexity of fly motoneurons. In this project I have looked at how the dendritic arbor is affected by changing the size of the target muscle.

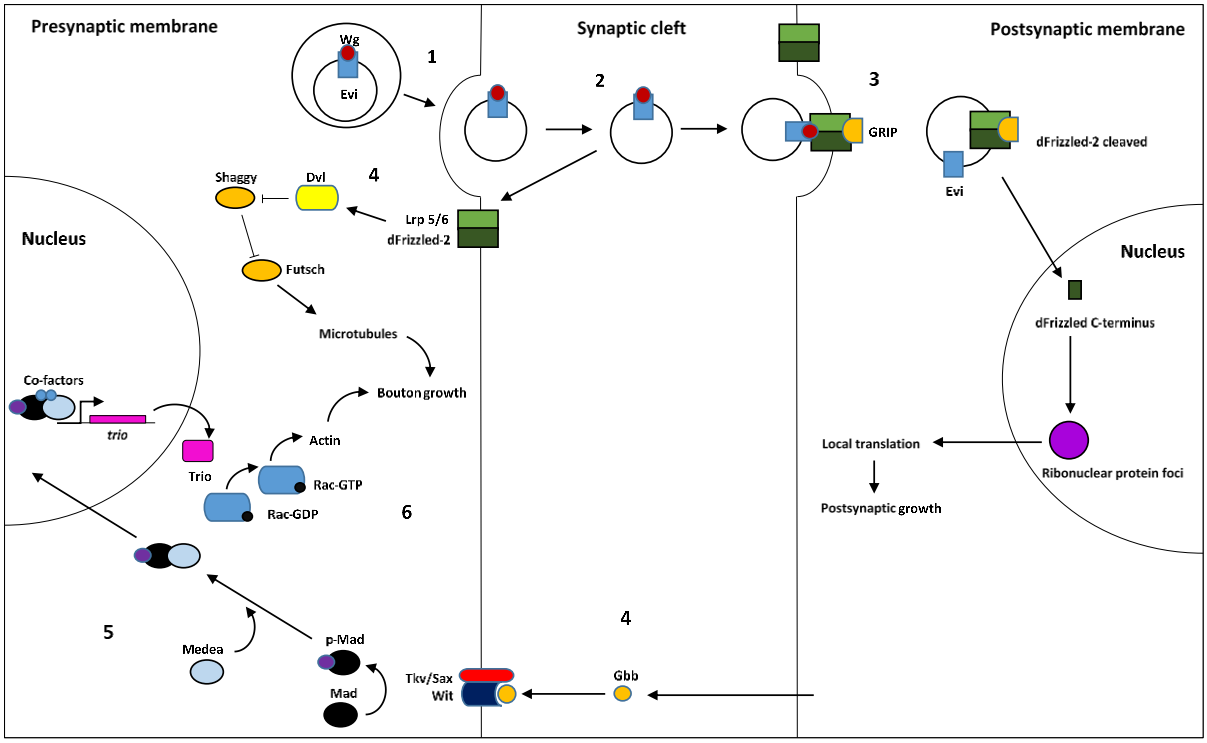

Fig 1. A schematic diagram summarising the *Wingless* (*Wnt*) and *Glass bottom boat* (*BMP*) signalling pathways at the *Drosophila* larval NMJ. (1) *Wg-Evi* complex is released in vesicles when the multi-vesicular body binds to the presynaptic membrane. (2) Postsynaptically *wg* binds to the *Lrp5/6-dFrizzled-2* receptor complex, and *Evi* facilitates the binding of *GRIP* to the receptor complex. The protein complex is endocytosed and *Evi* is necessary for trafficking the vesicles to a para-nuclear location where *dFrizzled-2* is cleaved, and the c-termini enter the nucleoplasm. These associate with large ribo-nuclear protein foci, containing synaptic protein transcripts, which are transported back to the postsynaptic membrane and locally transcribed. (4) *Gbb* is secreted postsynaptically and binds to the type II *wit* receptor, which in turn phosphorylates and activates the type I receptor, *Tkv* or *Sax*. (5) The cytoplasmic transcription factor *Mad* is phosphorylated, binds to *Medea*, and enters the presynaptic nucleus. In association with nuclear co-factors, the *pMad-Medea* regulates the transcription of genes such as *trio*.

1.4 Intrinsic factors

Internal programmes of transcription play a large part in determining the morphology of the dendritic arbor[89,90]. This is particularly obvious when different classes of neuron are grown in culture yet arborise in distinct patterns[91]. In some cases these differences are determined by a single transcription factor, while in other cases a large network is responsible for the different morphologies[91–93]. These transcriptional networks can influence many growth characteristics such as arbor growth rate, branching and guidance.

The accessibility of the *Drosophila* larval PNS has allowed researchers to investigate these intrinsic determinants of dendritic morphology. For example, *Hamlet* is a *Zn-finger* containing protein that acts as a binary switch between two peripheral neuronal cell fates with distinct morphologies - expression promotes the precursor cell towards an external sensory (*es*) cell fate rather than becoming a multiple dendrite (*md*) sensory neuron[94]. Over-expression of *Hamlet* can even revert *md* neurons to *es* neurons.

Unlike *Hamlet*, the dendrites of many other neurons are determined by the combined action of multiple transcription factors. Staying in the *Drosophila* PNS, the four sub-classes of *md* sensory neurons, the dendritic arborisation (DA) neurons, reach their final morphology from the combined action of *Cut, Abrupt* and *Spineless*. These genes act independently, which suggests that many transcriptional pathways act in parallel to determine the final shape of the dendritic arbor[95,96]. This is supported by work done by Parrish et al (2006) in which they identified around 70 transcription factors that regulate dendritic morphology of *Drosophila* sensory neurons[97].

Despite the diversity of adhesion molecules, transmembrane receptors, and signal transduction proteins expressed due to intrinsic transcription factors, the growth of the dendritic arbor is ultimately determined by changes to the actin and microtubule cytoskeleton[91]. Unsurprisingly intrinsic transcription factors regulate the expression of the *Rho* GTPases, known to influence dendritic morphology[98,99]. Other intrinsic cytoskeletal associated proteins such as *Kakapo* also determine arbor shape by crosslinking the actin and microtubule filaments. Mutations in *Kakapo* lead to a severely reduced dendritic arbor, as observed in the *Drosophila* sensory neurons[100].

1.5 External factors

The effects of external factors were originally studied with respect to axon guidance. However, the same signalling molecules often also determine dendritic outgrowth. Interestingly, the response of dendrites and axons to the same signalling molecule can be very different[101,102]. External cues can be long range, systemic signals that induce non-directional dendritic growth, such as the Ecdysone hormone, which acts as a read out of *Drosophila* larval size, and coordinates a concomitant increase in motoneuron dendrite length as the animal grows[36]. On the other hand signals can be shorter range and induce directional dendritic extension. *Semaphorin 3A* signals from the superficial layers of the vertebrate cortex induce outgrowth in the apical dendrites of the cortical pyramidal neurons towards the source of the signal[102,103].

Several studies investigating the effect of external factors on dendritic growth have focused on midline signalling in the *Drosophila* larva. This system demonstrates how the positioning of dendrites can be determined by a combination of different external factors, at times with opposing function. The appropriate medial-lateral positioning of the *Drosophila* larval RP3 motoneuron dendrites is determined by the attractive *Netrin* and repulsive *Slit* signals secreted from the midline. RP3s motoneurons have an ipsilateral and contralateral dendritic arbor, with the axon extending contralaterally. Mutation of the *Netrin* receptor, *Frazzled*, prevents the contralateral axon or dendrite from crossing the midline. On the other hand mutations in *Robo*, the *slit* receptor, cause the dendrites to grow into an abnormally medial position [104].

Dendritic growth relies on cytoskeleton organisation, though few studies have been able to demonstrate the direct connection between the binding of external signalling molecules and the internal pathways that lead to the rearrangement of actin and microtubules. Rosso et al (2005) showed that *Wnt7b* promoted dendritic outgrowth in cultured mouse hippocampal neurons by activating *Rac*[105]. This small *Rho*GTPase is involved in spine formation and initiates dendritic branching[98,106,107].

1.6 Activity

Neuronal activity has a large effect on the complexity and size of dendritic arbors. Early experiments demonstrated that rodents raised in a stimulus rich environment had significantly more complex cortical dendrites, possibly due to a greater level of excitation[108,109]. However, since then other studies have shown that separate classes of neurons respond differently to increased levels of excitation: in some cases dendrites extend, as for rodents in stimulus rich environments, while in others they retract. Likewise, monaural or monocular deprivation in rodents results in reduced and shifted dendritic arborisations in their respective neural pathways[59,110,111]. It seems that the model organism and the developmental stage play a large role in determining how a neuron's dendritic arbor will respond[112,113].

In the case of the *Drosophila* embryonic nervous system motoneurons appear to behave as homeostatic devices at a structural level. By increasing the density of presynaptic terminals available to the aCC motoneuron Tripodi et al (2008) showed a correlated reduction in the size of the dendritic arbor, and, conversely by removing synaptic transmission, they found that aCC motoneuron dendrites increased. These findings suggested that structural homeostasis is a mechanism to maintain a physiological level of depolarisation[113]. Larger arbors tend to synapse with more presynaptic interneurons, as was shown in the rabbit ciliary gangion cells[114]. It is this type of homeostatic mechanism that allows neuronal networks to be so robust in their output even though there is a relatively large amount of stochasticity in the system[115].

1.7 Myotopic Map

While motoneuron dendrites are highly dynamic structures their localisation within the dorsal neuropile is restricted to a particular anterior-posterior and medio-lateral position[26,116,117]. Motoneurons that innervate the same muscle domain (e.g. the dorsal-internal muscles) send their dendrites into similar regions of the neuropil. This dendritic segregation, called myotopic mapping, is independent of cell body position, and is believed to be an anatomical correlate of motoneuron connectivity and thus function[16].

Broadly speaking, there is an anterior-posterior segregation of dendrites from motoneurons innervating the internal (longitudinal) and external (transverse) muscles respectively. Additionally, motoneuron dendrites that innervate the internal muscles are further segregated along the medio-lateral axis: dendrites from motoneurons that target ventral muscles project more medially than those from motoneuons with dorsal muscle targets.

1.8 Aims of the Thesis

In this thesis I have used the *Drosophila* larval motor system to investigate how muscle size influences dendritic complexity of the innervating motoneurons. Specifically I have focused on the aCC motoneuron as it innervates only the DA1 muscle. In this way, any effect in the dendritic arbor due to a change in muscle size should be observable. The aCC motoneuron has a contralateral and ipsilateral arbor and is known to make connection with cholinergic, GABAergic and glutamatergic interneurons[28–30].

Muscle size was manipulated in one of two ways: either by driving *phosphoinosytol-3-kinase* or *cyclin E* in the target muscle. *Pi3Kinase* is a well know element in the insulin response signalling pathway and when over-expressed hypertrophies the cell[118–120]. On the other hand, maintained expression of *cyclin E* stops post-mitotic endoreplication, thus stunting muscle growth[121,122]. Using these transgenes introduced a large amount of variation in muscle size into the system, allowing me to observe whether there was a compensatory structural adaptation in the dendritic arbor of the very (aCC) motoneurons innervating these muscles.

2 Materials and Methods

2.1 Fly Strains

The following fly stocks were used in the experiments of this project: w^{-1118}, [RN2[123]-*Flp*][124] [hopA], [UAS-*Flp*], [*Tubulin84b*-FRT-STOP-FRT-*LexA*::VP16 [No5]], [LexAop-myr::*Cherry*], [pJFRC48-10xLexAOp2-IVS-myr::*tdTomato* in Su(Hw)attp5], [SS2M-*Gal4*][63], [UAS-*Flp*], [*Tubulin84b*-FRT-STOP-FRT-*Gal4*][125,126], [UAS-mCD8::*GFP*], [UAS-myr-*Pi3K*::CAAX(dp110)][127], [UAS-*CyclinE*]. Insertions were kept over [CyO, Dfd-GMR-*YFP*] or [TM6b, Sb, Dfd-GMR-*YFP*] balancer chromosomes (Bloomington Stock Center, Indiana University). All fly stocks used in this project were kept on a yeast-agar-cornmeal medium at room temperature (approx. 22°C).

2.2 Genotypes used

(A) w^{-}; SS2M-*Gal4*, UAS-*FLP*, *Tubulin84b*-FRT-CD2.STOP-FRT-*Gal4*, UAS-mCD8-*GFP*, pJFRC48-13xLexAOp2-IVS-myr::*tdTomato* in Su(Hw)attp5/ CyO, Dfd-GMR-*YFD*; RN2-*Flp* [hopA], *Tubulin84b*-FRT-STOP-*LexA*::Vp16 No5, LexAOp-myr::*Cherry*/ TM6b, Sb, Dfd-GMR-*YFP*; +

(B) UAS-myr-*Pi3K*::CAAX(*dp110*); +; +; +

(C) w^{-}; +; UAS-*CyclinE*; +

(D) w^{-1118}

The expression stock (A) was crossed to either (B), (C), or (D).

2.3 *Flippase* excision system

[RN2-*Flp*] is expressed transiently in the embryonic aCC and RP2 motoneurons. The stochastic action of the *flippase* in removing the stop codon (STOP) from [*tubulin84b*-FRT-STOP-FRT-*LexA*::VP16 No5, LexAop-myr::*Cherry*] means that RFP expression is maintained in a subset of aCCs and RP2s. Similarly, the [SS2M-*Gal4*] is expressed during embryonic development and is maintained through the action of [UAS-*Flp*], which removes the stop codon (STOP) from [*Tubulin84b*-FRT-CD2.STOP-FRT-*Gal4*].

Because both *Gal4* and *LexA* expression systems use a *flippase* to maintain their expression into larval stages, occasionally the *flippase* from one system will excise the stop codon from the alternative system. In these instances *Gal4* and GFP are expressed in the MNs while *LexA* and RFP can be expressed in the muscles. MNs expressing *Gal4* were not included in the study as they also express either *UAS-myrPi3kCAAX* or *UAS-Cyclin E*. Like the DA1 muscles these transgenes could influence MN cell size and obscure the effect of a retrograde signal on dendritic complexity[128].

The majority of MNs did not express Gal4 because of the different excision rates of the stop codons. The CD2.STOP codon from [*tubulin84b-FRT-CD2.STOP-FRT-Gal4*] is excised at a lower frequency than [*tubulin84b-FRT-STOP-FRT-LexA::VP16 No5*] due to it being a longer DNA fragment. Additionally, the location of the stop codons in the genome can influence the rate of excision.

2.4 Staging and dissection

Experimental crosses of adult flies were kept at 25^{o}C and were allowed to lay on plates containing an apple juice agar medium and yeast for 3 hours. Plates were then removed and moved to 29^{o}C for 57.6 hours. It was necessary to raise larvae at 29^{o}C as it increased the number of DA1 muscles expressing GFP. Presumably this was due to the increased activity of the Gal4 acting on the [UAS-*Flp*] and increasing the rate of stop codon splicing from the [*Tubulin84b*-FRT-CD2.STOP-FRT-*Gal4*], [UAS-mCD8::*GFP*]. Raising larvae at 29^{o}C decreases developmental time, therefore by 57.6 hours AEL the larvae had reached the third instar stage.

Larvae were developmentally staged and chosen for dissection by the shedding of the old cuticle. After removing any yeast, larvae were pinned ventral-side-up onto an inert Sylgard medium by head and tail (Austerlitz insect pins 0.10 mm stainless steel). Ultra-fine dissection scissors (Fine Science Tools) were then used to make an anterior to posterior cut along the ventral surface, allowing the removal of the viscera, tracheal tubes and the fat body. Further pins were used to secure the edges of the ventral cut such that the muscle field was stretched into a laminar sheet with the dorsal muscles at its centre. Dissections were performed in external saline ((in mM) 135 NaCl; 5 KCl; 4 MgCl2 • 6H2O; 2 CaCl2 • 2H_2O; 5 N-Tris[hydroxymethyl]methyl-2-amonoethanesulfonic acid; 36 sucrose (pH 7.15)) to prolong the life of the muscle field. After cutting the nerve roots and freeing the ventral nerve chord, it was then transferred onto a Poly-L-lysine coated coverslip. Double-sided tape was positioned either side of the VNC so that a protecting cover slip could be placed over the tissue. The aCC motoneuron dendrites are located in the dorsal neuropil so the VNC was orientated ventral-side-down (further details below). Throughout the poly-L-lysine coverslip the VNC remained bathed in electrophysiological saline.

2.5 Spinning disc confocal imaging and dendritic reconstruction

Immediately after dissection the VNC was viewed using a Yokagawa CSU-22 spinning disc confocal field scanner mounted on an Olympus BX51W microscope, through a 60x/1.2NA Olympus water immersion objective. RFP fluorescing aCC motoneurons were imaged if located in abdominal segments 3-6. The segmental body plan of the Drosophila larva corresponds to thoracic and abdominal segmentation in the VNC, with the most posterior neurons innervating the gut. Only motoneurons from segments 3 to 6 were chosen for imaging as they are considered to be most similar in terms of muscle and motoneuron morphology (M.Landgraf pers.comm). Motoneurons were not scanned if there were any neighbouring ipsilateral motoneurons fluorescing with RFP. The resolution of the confocal microscope is not high enough to distinguish between overlapping dendrites, thus making the subsequent reconstruction of the arbor impossible. Scanning an aCC motoneuron

involved taking a series of consecutive images along the z-axis (known as a z-stack), with a voxel size of 0.2x0.2x0.3µm.

Reconstructing the dendritic arbor was done using the Amira Resolve 5.3.3 (Visage Imaging, San Diego, USA) with an additional plugin (written by Dr F. J. Evers) specifically for modelling dendritic arbors [129,130]. Statistical algorithms allow the user to semi-automatically trace the dendrites in three dimensions.

2.6 Fixation

Before fixing specimens, the muscle field was imaged through the 63x water immersion objective of an axiophot upright wide-field fluorescence microscope (Zeiss). Because the RFP signal quickly photo-bleached and there was background RFP fluorescence in the samples, it was necessary to confirm the segment innervated by the aCC of interest. This ensured that the correct muscle could be subsequently scanned on the Leica SP5 confocal laser point scanning microscope (further details below). Muscle preparations were then fixed using with 4% formaldehyde (Fisher Scientific, Loughborough, UK) in Sorenson's saline (pH 7.2, 0.075M) for 15 minutes.

2.7 Staining and Mounting

Following fixation muscle preparations were permeabilised by three washes in Sorensen's containing 0.3% Triton-X-100 (Sigma-Aldrich, Dorset, UK) (PBT), before staining with primary and then secondary antibodies. The primary antibodies used in these experiments were *Mouse α-nc82* (The University of Iowa, Department of Biology, Iowa City, United States; 1:100) and *Goat α-HRP FICT 1:200* (Jackson ImmunoResearch, West Grove, PA, United States; 1:200). The monoclonal nc82 antibody specifically binds to *Bruchpilot*, an active zone associated structural protein, while antibodies against HRP label all neuronal tissue. After staining overnight at 5^{o}C, the primary antibodies were removed and the muscle preparations underwent three short and three long washes in PBT. Short washes lasted only a few seconds whereas long washes lasted 20 minutes. The same process of staining overnight at 5^{o}C, followed by three short washes and three

long washes in PBT was used with the secondary antibody, *Donkey α-mouse CF633* (Biotium, Inc.,Hayward,CA, United States, 1:600). Finally, the preps were left overnight in 70% glycerol : 30% saline before being mounted in *Vectasheild* (Vector Laboratories, Peterborough, UK). Mounting in *Vectashield* is preferable to glycerol as it stabilises the fluorphores, preventing photo-degradation.

2.8 Re-staining

Due to unforeseen problems with the stability of the CF633 conjugated secondary antibody in the Vectashield mounting medium it was necessary to repeat the staining process for all muscle preparations. This involved removing the muscle preparations from their slides, doing three short washes in PBT and then ten long washes in PBT (20 mins each). All the steps in section 2.7 were then repeated, the only difference being a new aliquot of *Donkey α-mouse CF633* secondary antibody.

2.9 Point scanning confocal microscope

Having stained active zones and neuronal tissue, the muscle preps were scanned with a Leica SP5 confocal laser point scanning microscope. Using the reference images taken with the Axiophot wide-field fluorescence microscope, the correct muscle could be identified and imaged, even when the RFP signal was very weak. The NMJ and active zones were scanned using a 63x/1.3NA glycerol immersion objective (Leica) whereas the whole muscle preparation was scanned using the 10x air (Leica) objective. Images taken with 10x objective allowed muscle areas to be measured for muscles DA1 and DO1.

2.10 Tracking larvae

A frustrated total internal reflection (FTIR) tracking system was used to assess the locomotion of larvae from each of the genetic treatments[20,131,132]. In this setup the edges of an agar-covered Perspex sheet are illuminated with infra-red (IR) LEDs. Because the IR waves are internally refracted, and the camera is placed below this Perspex sheet, the

background appears dark. The contact made by larvae allows the IR light to escape the Perspex-agar sheet, thus illuminating the animal's body.

Between 3 and 7 early third instar larvae were placed onto a 15cmx15cm agar sheet at any one time. The low density ensured that there were minimal collisions or larvae lost off the edge of the image. Like the dissections, larvae were raised at 29^{o}C for 57.6 hours and developmentally staged for the loss of the 2nd instar cuticle. A high definition camera was used to take a fifteen minute-long series of images at a rate of two images per second. The agar was maintained at 28-29^{o}C and changed every four scans to ensure that it did not dry out, as this influences larval locomotion. Genotypes were randomised with regard to their order in this sequence of four scans. Finally, FIMTrack v.2 software (Institute for Computer Science, University of Münster, Germany) was used to extract various features from the larval locomotion movies. The larvae from the different genotypes were compared on their average velocities. During tracking experiments larvae were unavoidably lost from the field of view. In some cases they returned to the stage, in which case the data from both paths could be combined. Larvae lost from the stage were only included if they featured in over half of the film.

2.11 Statistics.

One way analyses of variance (ANOVA) with Tukey's multiple comparisons test, and the linear regression analysis were carried out using Prism software (Graphpad Softare, CA, USA).

3 Results

3.1 Muscle manipulations

The aim of this thesis was to transgenically alter the size of the DA1 muscles to investigate whether there was a corresponding change in the dendrites of the innervating aCC motoneurons. This was achieved using the *Gal4*-UAS yeast expression system. An upstream SS2M promoter was used to restrict the expression of *Gal4* to DA1 muscles and they were visualised using a *UAS-mCD8-GFP* reporter (**Fig 2A**). By crossing-in either the *UAS-myristoylated-PI3-kinase* or *UAS-cyclin E* reporters, the objective was to increase and decrease muscle area respectively. *Pi3-kinase* is a well characterised element in the insulin signalling pathway with many downstream effectors, including those that regulate cell growth. Increasing expression of *Pi3K* induces hypertrophy[119,133]. On the other hand, maintained expression of *Cyclin E* stunts muscle growth by preventing consecutive rounds of non-mitotic endoreplication[121].

Third instar larvae were developmentally staged by the shedding of their old cuticle and mouth hooks. Following dissection each muscle preparation was fixed, stained, mounted and imaged using the SP5 point scanning confocal microscope.

While the transgenes had a clear and significant effect on muscle size (One-way ANOVA, $P \leq 0.0001$) (**Fig 2B**), there was also a noticeable variability in the size of the third instar larvae. To quantify this variability I measured the average area per animal of DO1 muscles, which are adjacent to the *Gal4* expressing, genetically manipulated muscles, but which themselves did not express *Gal4* or the *Gal4* reporter *UAS-mCD8::GFP*. The DO1 muscles are located internally relative to the DA1 muscles (**Fig 2A**) and variability in DO1 muscle size did not correspond to genotype (One-way ANOVA, $P>0.05$) (**Fig 2C**). Instead DO1 muscle area correlated with the total length of the abdominal segments 3-6 (Linear regression analysis, $P<0.0001$) (**Fig 3A**). Thus, DO1 muscle area could be used as an indicator of animal size and used to normalise specimens for specimen-specific differences in animal size. The full effect of transgene expression on DA1 muscle size was determined by the ratio between the average area of *Gal4*-expressing DA1 muscles and

the average area of *Gal4*-negative DO1 muscles in that very specimen. By taking overall larval size into account the effect of transgene expression on DA1 muscle size became apparent (One-way ANOVA, P<0.0001) (**Fig 2D**).

There is a linear relationship between the average area of DA1 muscles expressing *Gal4* and the average area of *Gal4*-negative DO1 muscles (**Fig 3B**) across all genotypes.

Fig 2. UAS-myrPi3K CAAX and UAS-Cyclin E have opposing and significant effects on muscle size.

(A) Composite bright field-fluorescence images showing the orientation of non-fluorescent DO1 muscles (outlined in white) and fluorescent DA1 muscles (outlined in navy blue) in fillet preparations of larvae from the three genetic treatments. DA1 muscles express either *UAS-myrPi3k CAAX (*top), *UAS-cyclin E* (bottom), or are from the control group (middle). In all images the midline runs from top right (anterior) to bottom left (posterior). (B) Per larva average area of DA1 muscles expressing Gal4, (C) per larva average area of DO1 muscles not expressing *Gal4*, (D) per larva ratio of average DA1 muscle area expressing *Gal4*/average *Gal4*-negative DO1 muscle area, plotted against genetic treatment. (B), (C) and (D) Mean ± range. One-way ANOVA (B, P≤0.0001; C, P>0.05; D, P≤0.0001) and Tukey's multiple comparisons test (ns P>0.05; * P≤0.05; ** P≤0.01; *** P≤0.001; **** P≤0.0001).

(Next page)

Fig 2

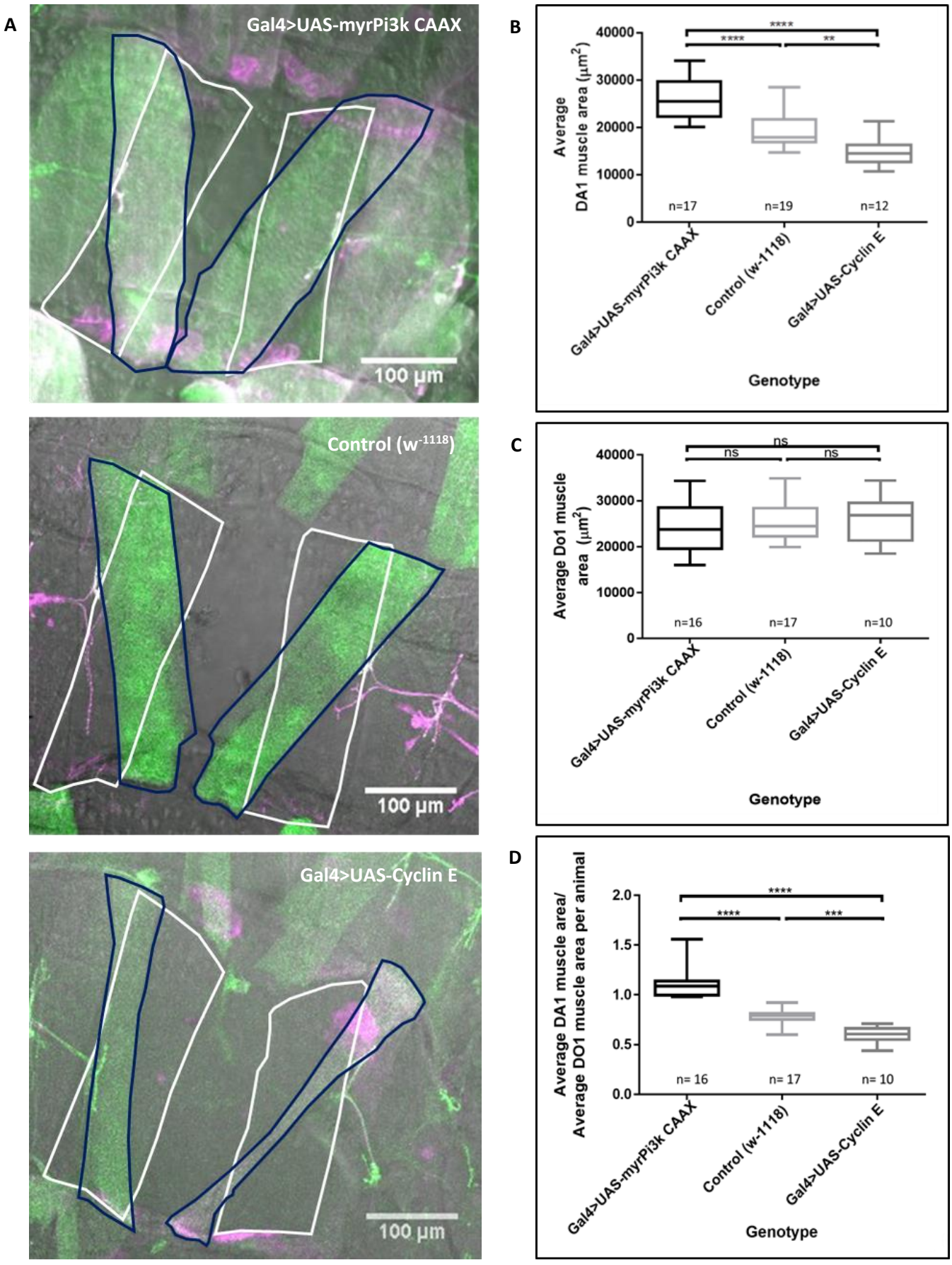
A
Gal4>UAS-myrPi3k CAAX
100 µm
Control (w-1118)
100 µm
Gal4>UAS-Cyclin E
100 µm
B
Average DA1 muscle area (µm2)
40000
30000
20000
10000
0
****
****
**
n=17
n=19
n=12
Gal4>UAS-myrPi3k CAAX
Control (w-1118)
Gal4>UAS-Cyclin E
Genotype
C
Average Do1 muscle area (µm2)
40000
30000
20000
10000
0
ns
ns
ns
n=16
n=17
n=10
Gal4>UAS-myrPi3k CAAX
Control (w-1118)
Gal4>UAS-Cyclin E
Genotype
D
Average DA1 muscle area/ Average DO1 muscle area per animal
2.0
1.5
1.0
0.5
0.0
****
****
***
n= 16
n= 17
n= 10
Gal4>UAS-myrPi3k CAAX
Control (w-1118)
Gal4>UAS-Cyclin E
Genotype

Fig 3

A

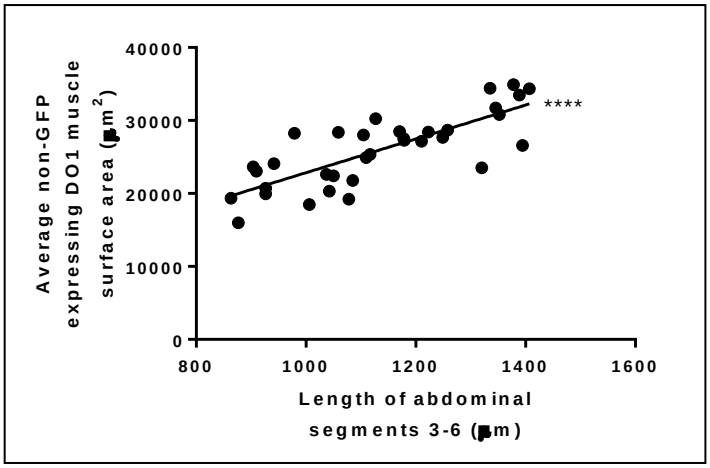

B

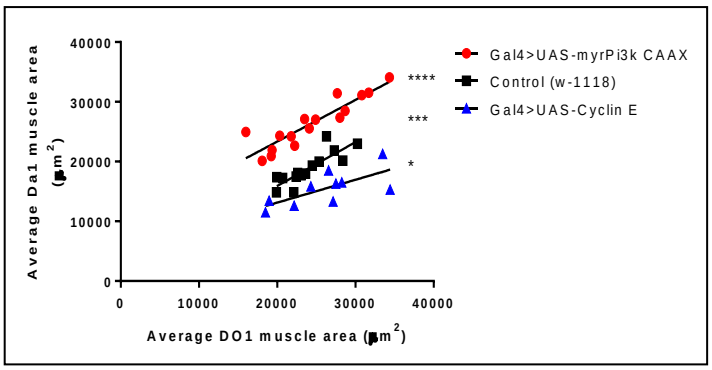

Fig 3. DO1 muscle surface area can be used as a proxy of animal size, and therefore used to normalise DA1 muscle area across all genotypes. A positive correlation exists between the length of abdominal segments 3-6 and DO1 muscle surface area (Fig 3A). There is also a positive relationship between the average area of Gal4-negative DO1 and Gal4-expressing DA1 muscles for larvae expressing *UAS-myrPi3K CAAX* (red circles), *UAS-cyclin E* (blue triangles), or control larvae (black squares) (Fig 3B). Black line shows linear regression analysis. Asterisks represent where the slope of the regression deviates significantly from zero (* P≤0.05; ** P≤0.01; *** P≤0.001; **** P≤0.0001).

3.2 Dendritic arbor reconstructions

During the dissection of the third instar larvae the ventral nerve chord was removed, viewed with a spinning disc confocal microscope, and scanned if an aCC motoneuron in an appropriate abdominal segment was fluorescing with RFP. Scanning the nerve chord involved taking a sequence of images in the z-axis such that the dendritic arbor could be reconstructed at a later date. aCC motoneurons were visualised with another yeast transcription factor, *LexA*, and its binding site, the *LexA operon* (*LexAop*). The RN2 promoter restricted the expression of *LexA* to the aCC and RP2 motoneurons, and the *LexAop-myr::td-Tomato* and LexAOp-myr::*Cherry* reporters facilitated their visualisation. aCC motoneurons were only scanned if they were found in abdominal segments 3-6 and did not have fluorescing motoneurons in neighbouring segments, i.e. only if physically distinct and not overlapping with any other fluorescently labelled neurons.

Reconstructions were done using Amira 5.3.3 with an additional plug-in specifically written for modelling dendritic arbors (written by Dr Jan Felix Evers). A core branch was considered to be the length of reconstruction in between two branch points, while the terminal branches (tips) were the lengths of arbor following a single branch point and themselves having no further branch points or branches. Because studies have shown that the growing tips of an arbor are highly motile filopodia that have not yet been stabilised with the microtubule cytoskeleton, the terminal segments have been considered separately from the rest of the arbor. In the following paragraphs I refer to the reconstruction without terminal segments as the 'core arbor' and the sum of the terminal segments as the 'terminal arbor'. aCC motoneurons have two sets of dendrites: an ipsilateral arbor that branches from a region of the axon, and a contralateral arbor that extends from the soma and across the midline (**Fig 4A,B**). When reconstructing the ipsilateral arbor I have excluded from the dendritic arbor analysis the primary neurite as this also functions as an axon (**Fig 4C**).

Due to variation in larval size at the third instar stage it was necessary to normalise the lengths of the core arbor and the area of the DA1 muscles with respect to individual animal size. To do this the average area of the non-fluorescing (*Gal4*-negative) DO1 muscles **per larva** was divided by the average area of DO1 from **all larvae** from all

treatments. This gave an index of relative larval size, such that a larva smaller than average would have a value <1, while a larger than average larva would have a value >1. To normalise DA1 muscle area and core arbor length, both were then divided by this index.

Once normalised to the size of the animal, there is a correlation between DA1 muscle area and the length of the aCC core arbor (Linear regression analysis, P=0.0171) (**Fig 4D**). On closer inspection this correlation occurs between DA1 muscle area and the contralateral core arbor length (Linear regression analysis, P=0.0184) (**Fig 4E**). There does not appear to be a statistically significant effect in the ipsilateral core arbor. However, there is a significant correlation between the lengths of the core ipsilateral and the core contralateral arbors (Linear regression analysis, P=0.0098) (**Fig 4F**) suggesting that larger dendritic trees are larger both in terms of their ipsi- and their contralateral dendritic sub-arbors. It also suggests that there may be a more subtle effect on the ipsilateral arbor, which does not show as statistically significant difference between the different DA1 muscle treatments, at least with the current sample size. **Fig 5** shows aCC MNs with core arbors of various sizes, lying close to the regression line of **Fig 4D.**

Following normalisation, there was also a significant positive correlation between the contralateral terminal arbor (dendritic tips only) and DA1 muscle area (Linear regression analysis, P=0.0044) (**Fig. 6A**). No such effect was observed in the ipsilateral terminal arbor (dendritic tips only). Similar to the core arbor, when focusing on the dendritic terminal (tip) segments only, there is also a positive correlation between the ipsilateral and contralateral terminal arbors (dendritic tips only) (Linear regression analysis, P=0.0128) (**Fig. 6B**). Again, this could suggest a subtle change in the terminal dendrites of the ipsilateral arbor that is concomitant with manipulation of DA1 muscle size.

Fig 4

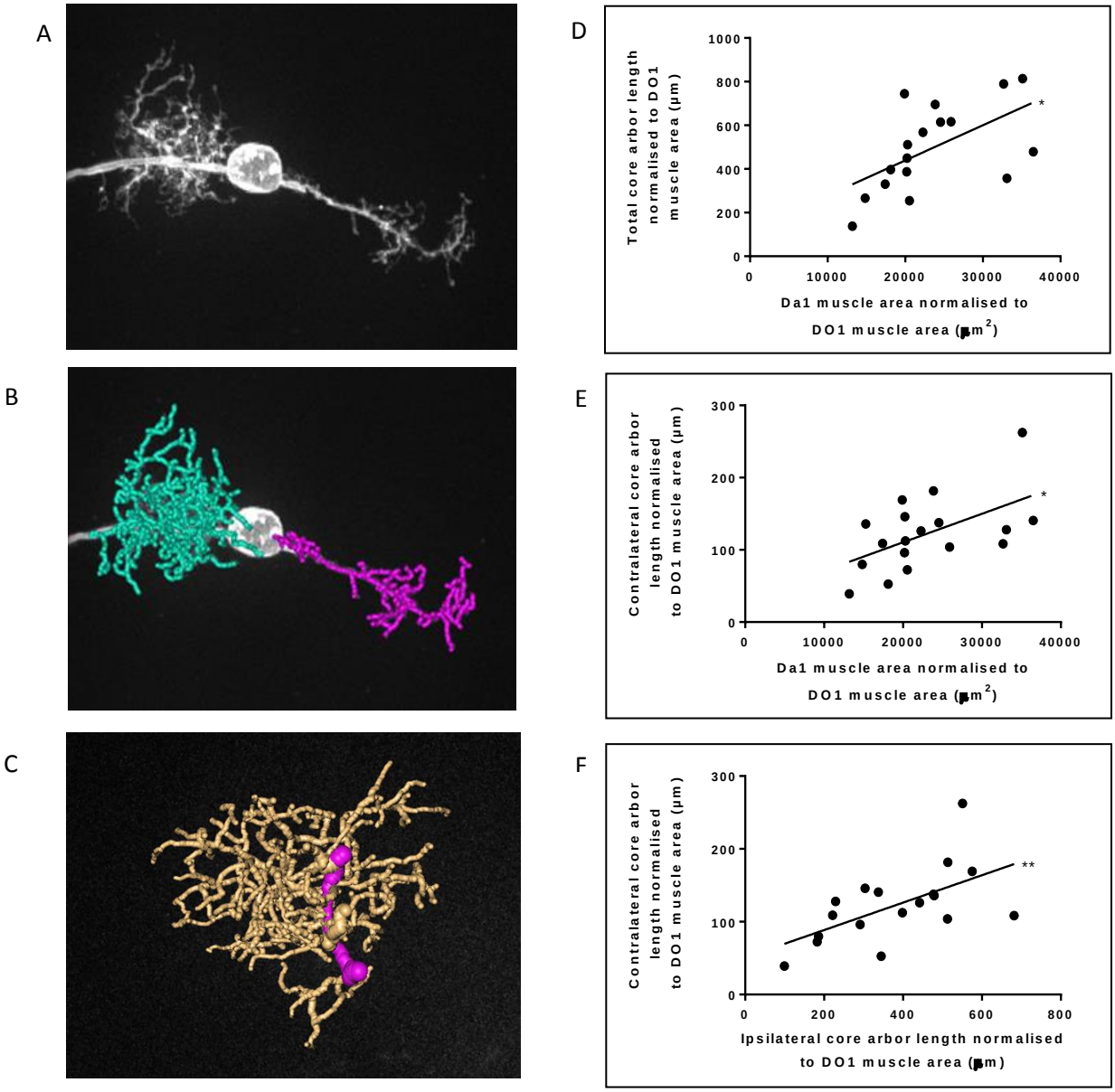

Fig 4. Contralateral core arbor length correlates with DA1 muscle size when both variables are normalised with regards to larval size.

(A) Z-projection of an aCC motoneuron. (B) 3D reconstruction of an aCC motoneuron superimposed on top of a z-projection. Ipsilateral arbor highlighted in turquoise, contralateral in pink. (C) Ipsilateral reconstruction with the primary neurite highlighted in pink. To take into account animal-specific differences in size in (D), (E) and (F), DA1 muscle area and aCC core arbor length were divided by an index of animal size. This index is calculated by dividing the average area of the non-fluorescing (*Gal4*-negative) DO1 muscles **per larva** by the average area of DO1 from **all larvae** from all treatments. (D) Correlation between the total core arbor length and DA1 muscle area when both variables are divided by the index of animal size. (E) Correlation between the contralateral core arbor length and DA1 muscle area when both variables are divided by the index of animal size. (F) Correlation between normalised core lengths of the contralateral and ipsilateral arbors. Black line in (D), (E) and (F) shows linear regression analysis. Asterisks represent where the slope of the regression deviates significantly from zero (* P≤0.05; ** P≤0.01).

Fig 5

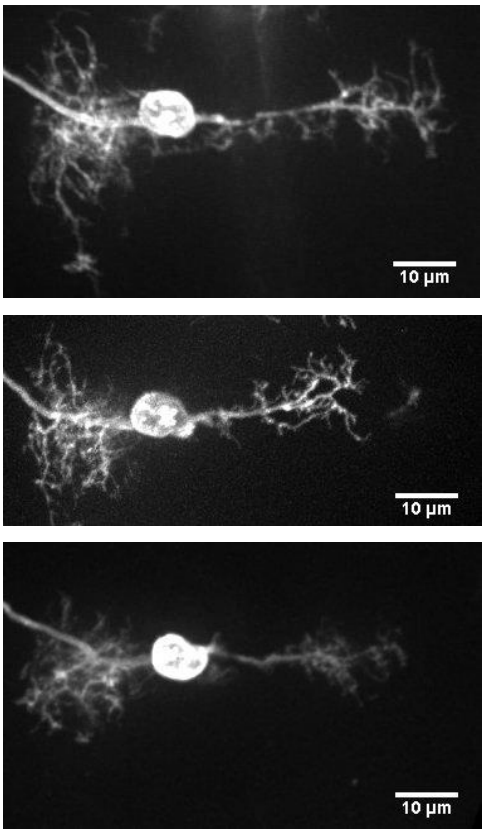

Fig 5. Z-projections of aCC MNs with a large (top), medium (middle), and small (bottom) core dendritic arbors, lying close to the regression line in Fig 4D.

Fig 6

A

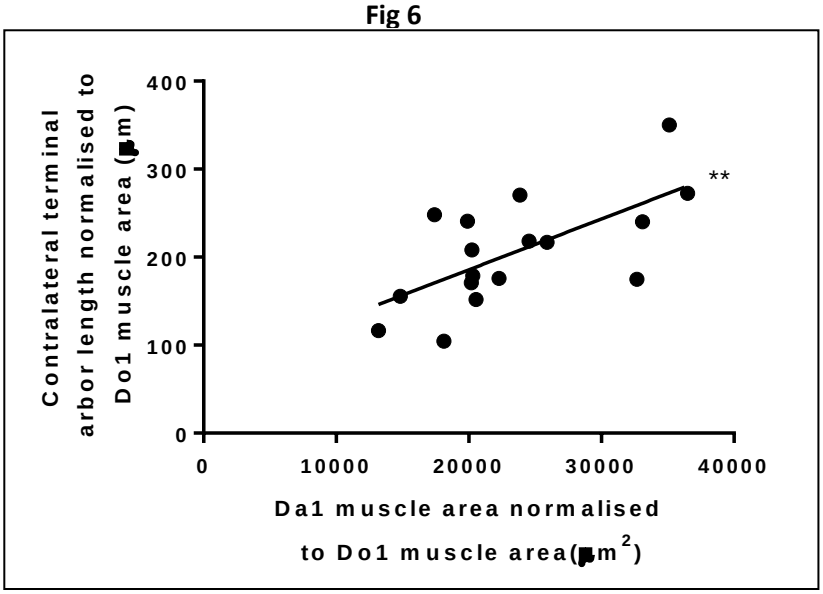

B

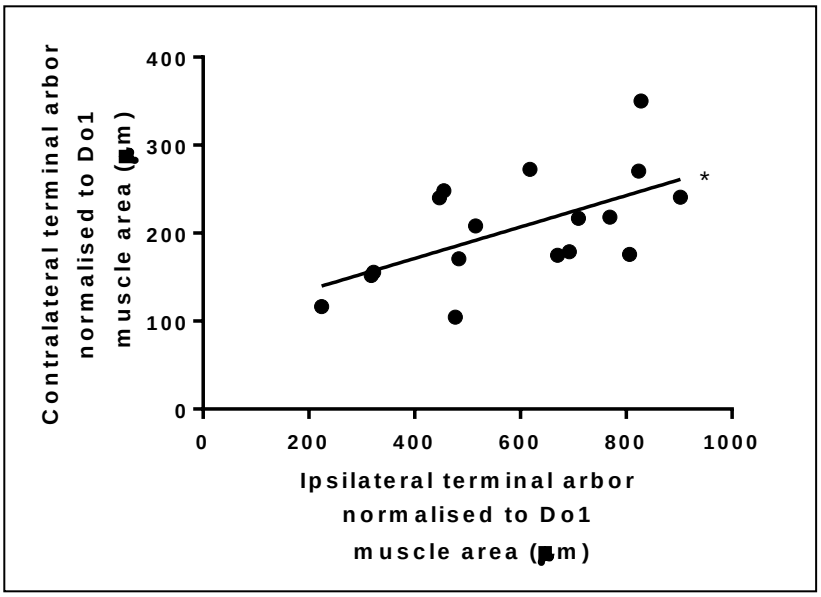

Fig 6. **Contralateral terminal arbor length correlates with DA1 muscle size when both variables are normalised with regard to DO1 muscle size.**

(A) Positive correlation between DA1 muscle area and contralateral terminal arbor length, when both are normalised to DO1 muscle area. (B) Also a positive correlation between normalised ipsilateral and contralateral terminal arbors. Black line shows a linear regression analysis. Asterisk indicates that the slope of the regression deviates significantly from zero (* P≤0.05; ** P≤0.01).

3.3 Branch length

The size variation in the reconstructed arbor lengths could be due to differences in branch length, branch number, or a combination of both. Core branch length is relatively constant, at approximately 2µm, and is independent of whether branches were measured in the ipsilateral or contralateral core arbors (**Fig 7A**). The average length of terminal segments is longer (approx. 4µm) and also more variable than the core segments (**Fig 7B**). There is a significant negative correlation between the average length of ipsilateral terminal segments and the ipsialteral core arbor length (Linear regression analysis, P=0.0037) (**Fig 7B**): a larger core dendritic tree appears to have shorter terminal segments. This does not mean that the total length of the ipsilateral terminal arbor is reduced. **Fig 7C** shows the tight positive relationship between core and terminal arbor lengths. Thus, while larger ipsilateral core arbors have a proportionally larger total terminal arbor length, the average length of the terminal segments is shorter (**Fig 7D**).

The significant difference between core and terminal branch lengths is observed across all genotypes (One-way ANOVA, P<0.0001) (**Fig 8**). Core branch length is also consistent across genotypes (**Fig 8**), suggesting that variation in dendritic tree size is due to differences in core branch number. **Fig 9** demonstrates that there is a positive relationship between core arbor length and the number of constituent branches.

Fig 7. Mean core arbor segment length is approximately 2µm.

(A) Average core segment length, (B) Average terminal segment length, of ipsilateral (green circles) and contralateral (pink triangles) arbors plotted against total core arbor length. (C) The positive correlation between the core and terminal arbor lengths. (D) Average terminal segment length in ipsilateral (green circles) and contralateral (pink triangles) arbors plotted against total length of terminal segments. Black line in (A), (B) and (C) shows linear regression analysis. Asterisks represent where the slope of the regression deviates significantly from zero (* P≤0.05; ** P≤0.01; *** P≤0.001; **** P≤0.0001).

Fig 8. Core branch length does not differ significantly between genotypes. Mean ± range. One-way ANOVA (P≤0.0001) and Tukey's multiple comparison's test with asterisks indicating significance (* P≤0.05; ** P≤0.01; *** P≤0.001; **** P≤0.0001).

Fig 9. Longer core arbors are due to more branches.

Tight correlation between the total length and the number of segments in the core arbor. Black line shows linear regression analysis. Asterisk represents a slope where the regression significantly deviates from zero (**** P≤0.0001).

Fig 7

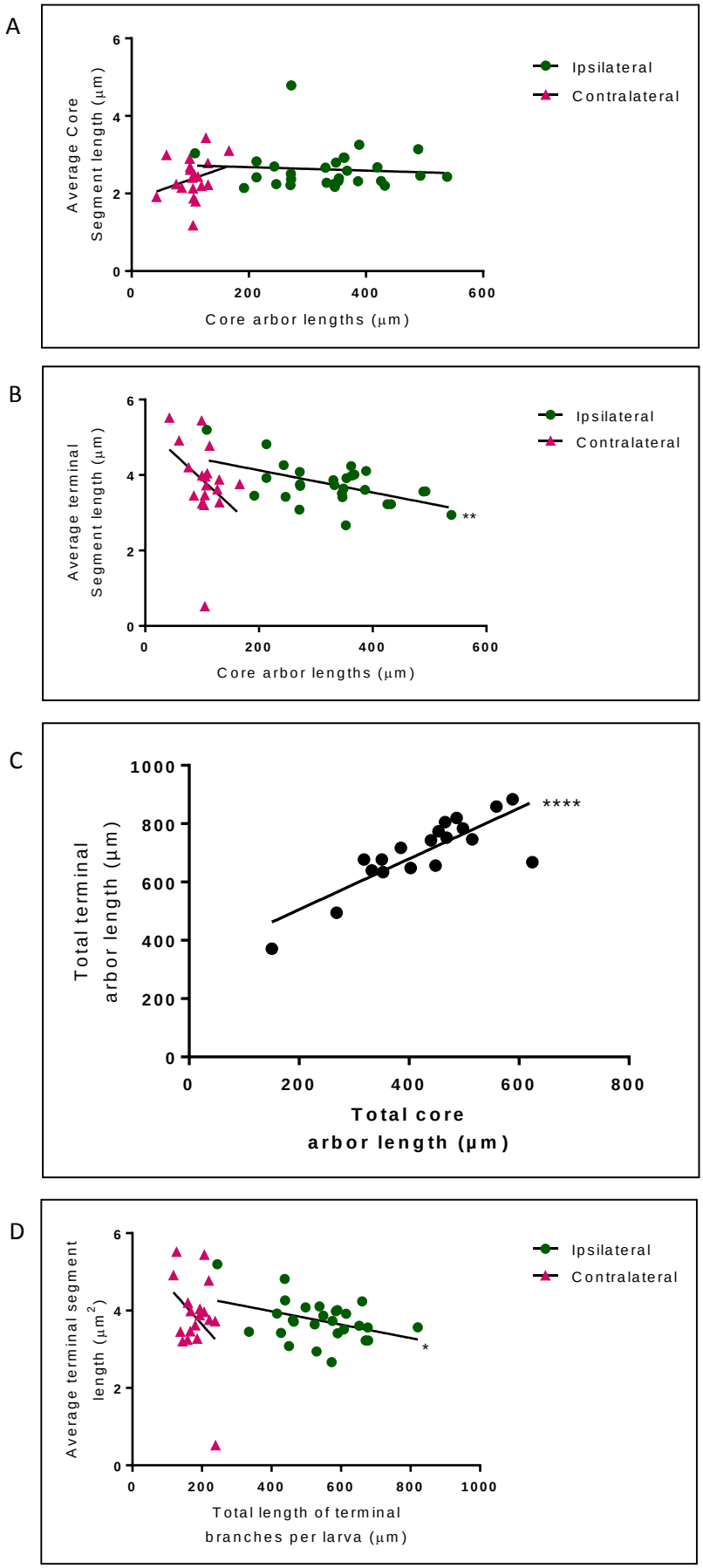
A
Average Core Segment length (µm)
Core arbor lengths (µm)
Ipsilateral
Contralateral
B
Average terminal Segment length (µm)
Core arbor lengths (µm)
**
C
Total terminal arbor length (µm)
Total core arbor length (µm)
****
D
Average terminal segment length (µm2)
Total length of terminal branches per larva (µm)
*

Fig 8

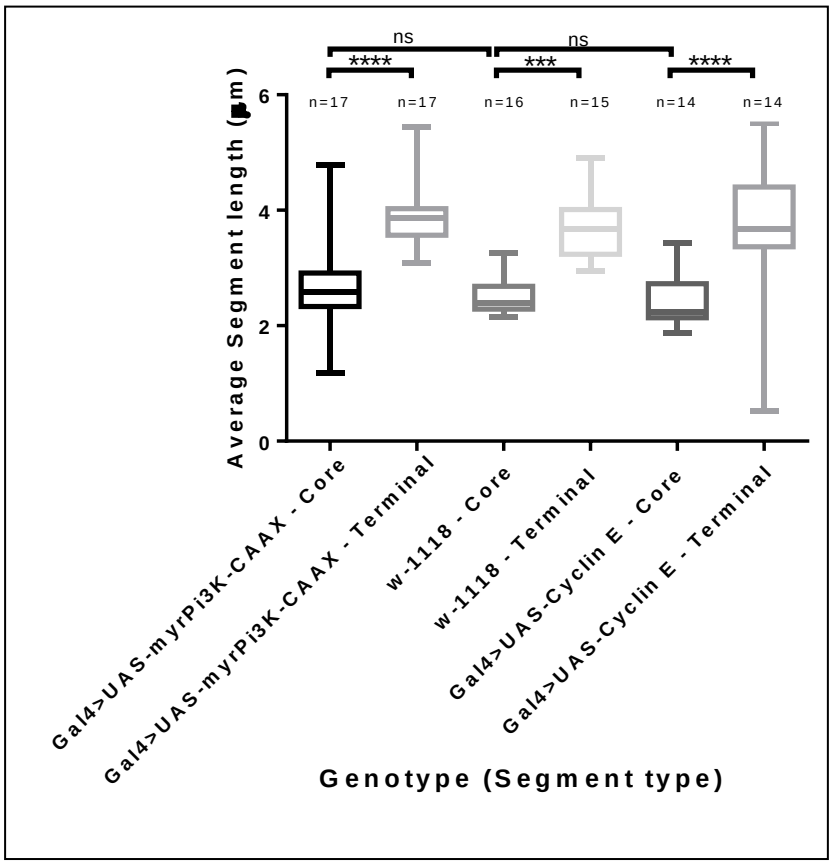
ns
ns
****
***
****
n=17
n=17
n=16
n=15
n=14
n=14
Average Segment length (µm)
0
2
4
6
Gal4>UAS-myrPi3K-CAAX - Core
Gal4>UAS-myrPi3K-CAAX - Terminal
w-1118 - Core
w-1118 - Terminal
Gal4>UAS-Cyclin E - Core
Gal4>UAS-Cyclin E - Terminal
Genotype (Segment type)

Fig 9

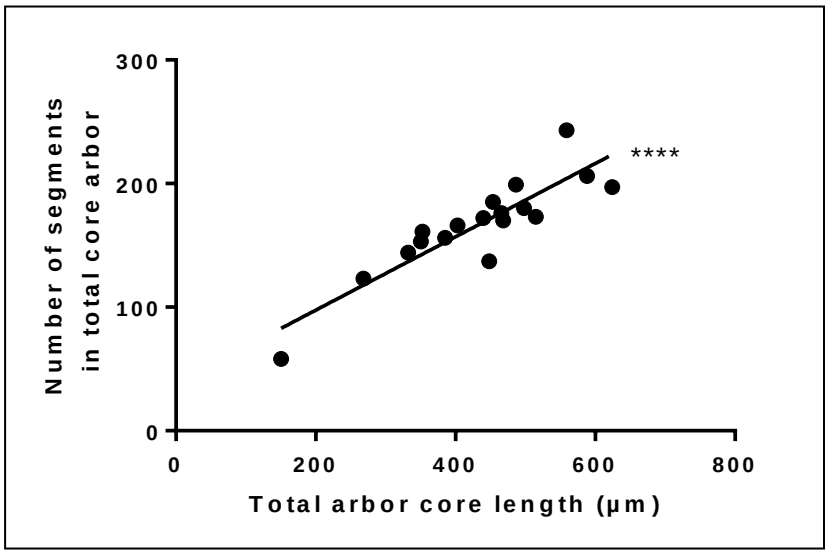
Number of segments in total core arbor
0
100
200
300
****
0
200
400
600
800
Total arbor core length (µm)

3.4 Sholl Analysis

Sholl analysis is a method of quantifying the distribution of dendritic branches in space. This technique first involves defining the primary neurite and then on top of this superimposing concentric 3D layers that mirror the primary neurite's shape. The layers are 2µm in width and subdivide the volume of space encompassing the arbor. Using the Amira (5.3.3) software I was able to measure the length of arbor and number of branch-points in each 2µm-wide layer.

Defining the primary neurite is an important aspect of Sholl analysis. This is particularly difficult in the contralateral arbor as there is no clearly definable axon from which the dendrites develop, unlike the ipsilateral arbor. For this analysis I defined the contralateral primary neurite as the brightest and straightest neurite extending from the soma to the most distal position in the arbor. It was important to be consistent in defining the primary neurite as it determines the shape of the Sholl analysis. While the ipsilateral arbor has a bell-shaped distribution of branch length (**Fig 10A**) and number of branch points (**Fig 10B**) away from primary neurite, the contralateral arbor has a very different shape. There is a small peak in the number and length of contralateral branches at around 3µm, with a subsequent decrease at greater distances from the primary neurite (**Fig 10C, 10D**).

Fig 10. There is a marked difference in the shape of ipsilateral and contralateral Sholl analyses.

(A) and (C) Sholl analyses showing the sum of dendritic length as a function of distance from the ispilateral and contralateral primary neuritis, respectively. (B) and (D) Sholl analysis of the number of branchpoints as a function of distance from the ispilateral and contralateral primary neurites respectively. For each graph: red circles - Gal4>UAS-myrPi3K CAAX, blue triangles – Gal4>UAS-Cyclin E, black squares – control (w-1118). Mean± SEM.

(Next page)

Fig 10

A

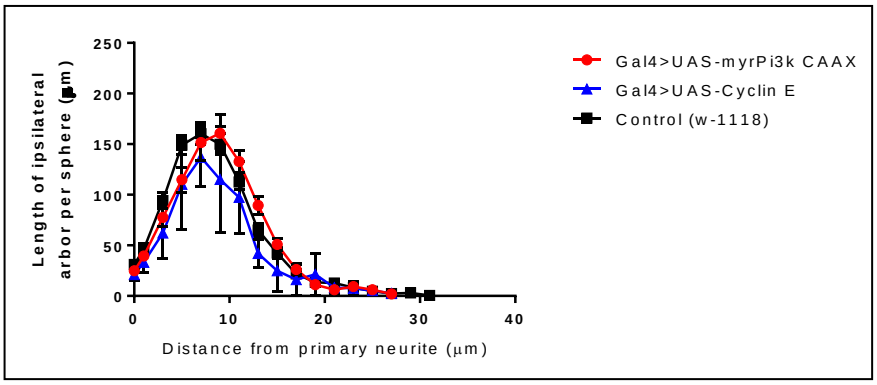
Length of ipsilateral arbor per sphere (µm)
250
200
150
100
50
0
0
10
20
30
40
Distance from primary neurite (µm)
Gal4>UAS-myrPi3k CAAX
Gal4>UAS-Cyclin E
Control (w-1118)

B

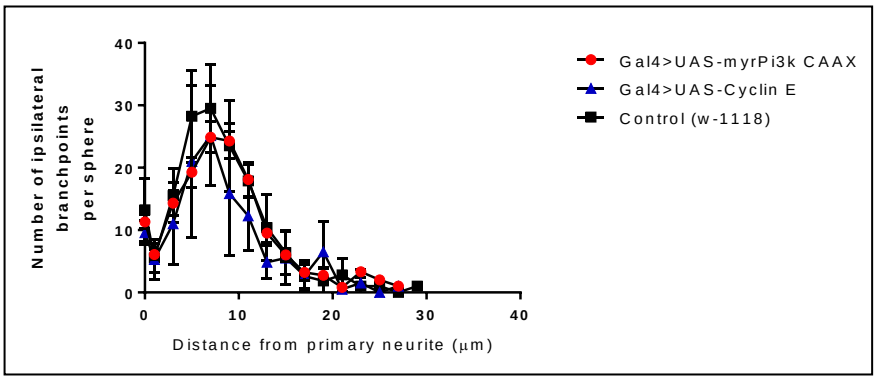
Number of ipsilateral branchpoints per sphere
40
30
20
10
0
0
10
20
30
40
Distance from primary neurite (µm)
Gal4>UAS-myrPi3k CAAX
Gal4>UAS-Cyclin E
Control (w-1118)

C

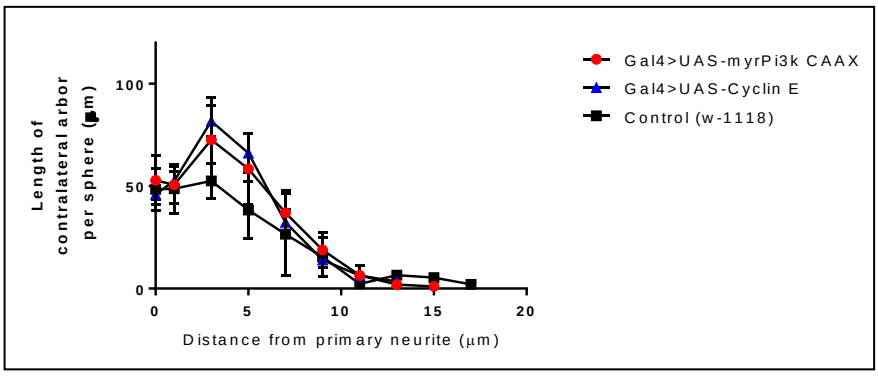
Length of contralateral arbor per sphere (µm)
100
50
0
0
5
10
15
20
Distance from primary neurite (µm)
Gal4>UAS-myrPi3k CAAX
Gal4>UAS-Cyclin E
Control (w-1118)

D

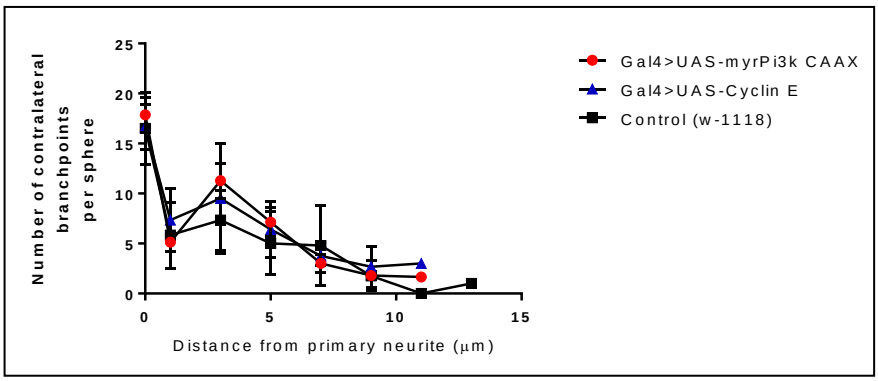
Number of contralateral branchpoints per sphere
25
20
15
10
5
0
0
5
10
15
Distance from primary neurite (µm)
Gal4>UAS-myrPi3k CAAX
Gal4>UAS-Cyclin E
Control (w-1118)

3.5 Tracking Larvae

A potentially confounding factor in this study is that the genetic backgrounds of each treatment is altering larval behaviour. A change in locomotor network activity could also influence motoneuron dendrite size[134]. To examine this possibility, I decided to study the larval crawling velocity. Also, by tracking the larvae it was possible to determine whether the disproportionate DA1 muscle size was having a significant effect on locomotion. The early third instar larvae used in this project exhibited foraging behaviour, characterised by a series of forward crawls separated by pauses and turns[135]. Many factors can influence locomotor behaviour, including temperature, the texture of the surface, humidity, genotype and age. **Fig. 11** demonstrates that the average velocity of larval locomotion was comparable across genotypes (One-way ANOVA, P>0.05).

Fig 11

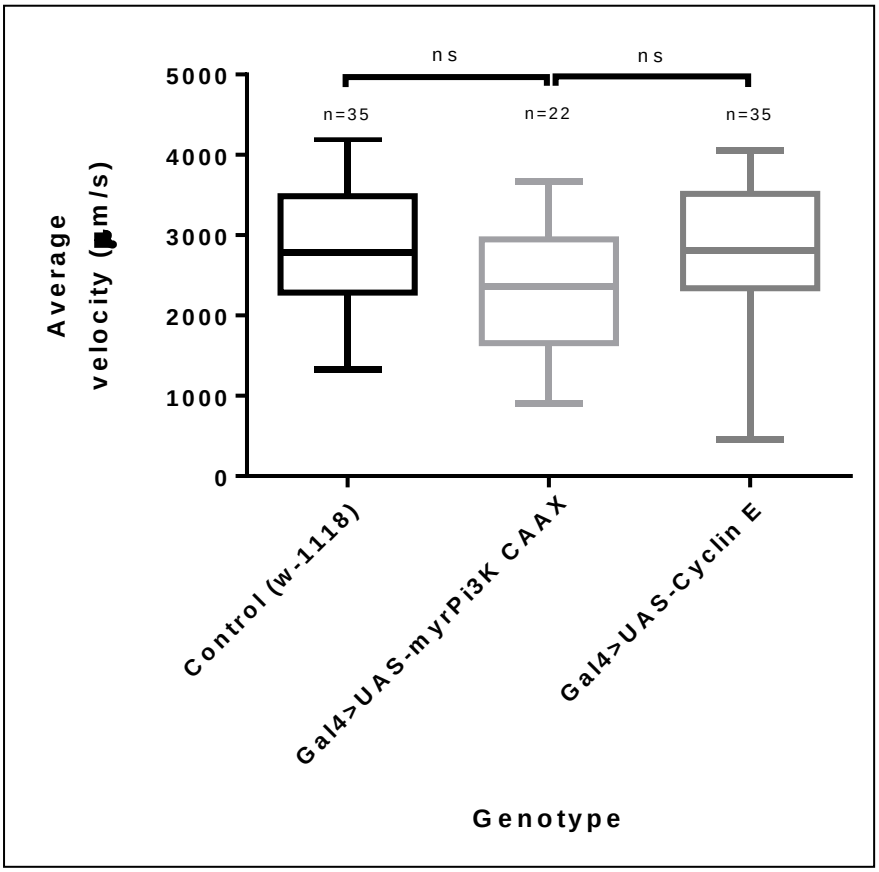

Fig 11. Genotype has no effect on larval locomotion. Average velocity plotted against genotype. Mean± range. One-way ANOVA (P>0.05) and Tukey's multiple comparisons test (ns P>0.05).

4 Discussion

The results in this thesis build on work done by Dr Maarten Zwart (2012). His preliminary results suggested that dendritic arbors may be influenced by muscle derived retrograde signals. In this thesis I have presented my results investigating whether DA1 muscle area correlates with dendritic arbor length. The hypothesis is that a larger muscle requires greater synaptic drive, as the input resistance is decreased. Zwart et al (2013) demonstrated that a larger arbor makes more contacts with presynaptic interneurons, receives a larger synaptic drive, and has more action potentials during bursts of activity. Thus by growing a larger dendritic arbor, the motoneuron can increase its synaptic drive and thus lengthen its activity burst periods to compensate for size-associated changes in muscle physiology. That way the motoneuron-muscle unit is capable of maintaining physiologically appropriate levels of muscle depolarisation as the animal grows.

4.1 Visualising the DA1 muscles and aCC motoneurons

To conduct my experiments I constructed a fly stock in which a specific muscle (DA1) and its innervating motoneuron (aCC) could both be visualised at the same time with different fluorphores and manipulated independently of one another. Briefly, in this stock *Gal4* expression was targeted to DA1 muscles, visualised with *UAS-mCD8::GFP*, and *LexA::VP16* expression was targeted to aCC (and RP2) motoneurons, visualised with *13xLexAop2-IVS-myr::td-Tomato* inserted in *Su(Hw)attp5* reporters. This stock ensured that *Gal4* expressing muscles fluoresced green and some of their innervating aCC motoneurons red. I crossed transgenes to this experimental expression stock and showed that muscle area could thus be increased and decreased. I then measured motoneuron dendritic arbor size to infer whether a retrograde signal could determine dendritic development.

Having different yeast transcription factor expression systems in the muscle and motoneuron has the advantage of avoiding invasive and potentially confounding procedures. Much of the early research investigating the role of retrograde signalling was done by ablating the axons of ganglion cells in the SCG, thus disconnecting a neuron from its target cell[1–3]. More recently, experiments with the RP2 motoneurons of the *Drosophila*

larva looked at the effects of laser axotomy (Zwart, unpublished). In such studies the motoneuron dendritic arbor retracted [1,2]. While the authors argue that axotomy is unlikely to cause a significant cell-damage response[78,79], it is hard to imagine that the neuron does not react at all to such a large loss of membrane. There are many physiological responses to axotomy[136,137], and the observed dendritic retraction could be a side effect of axon reorganisation.

4.2 Contralateral core arbor

In this thesis I have shown that DA1 muscle size is significantly affected by both *Cyclin E* and *dp110 (Pi3K)* expression. I have also demonstrated that there is considerable variation in the size of larvae as they reach the third instar stage. This variation is consistent across genotypes suggesting that the effector transgenes were not having a global effect on larval size. Dendritc arbor length increases as the animal grows. Zwart et al (2013) showed that arbor length greatly increased with the age of the *Drosophila* larva, from the early first to early third instar[36]. While their study did not specifically compare animal size with arbor length, older animals are larger. It therefore seems reasonable to assume that size variations in larvae at the same developmental stage could have corresponding differences in arbor length. To see the effect of retrograde signalling it was therefore necessary to normalise both aCC motoneuron dendritic arbor length and DA1 muscle area to the DO1 muscle area, a proxy of animal size. When normalising dendritic arbor length I separated the core and terminal branches (dendritic tips), as the latter are generally believed to be highly motile filopodia and with their transient exploratory nature may therefore introduce a great deal of variability (M.L. & J.F. Evers, pers.comm.). This decision was also partly based on my own reconstructions of ipsilateral and contralateral arbors, in which the core branches are consistently around 2µm, while the terminal branches are on average longer and more variable in length.

Normalising DA1 muscle area and dendritic arbor length revealed a positive correlation between the length of the aCC contralateral core arbor and DA1 muscle area. This suggests that in animals, in which the DA1 muscle size has been genetically manipulated, the neuron is changing its dendritic tree size to adjust to a muscle that is out of

proportion with the rest of the animal. Retrograde signals act as a means of communication between post and presynaptic cells. A muscle that is out of proportion with the rest of the animal will likely receive a synaptic drive that is either too large or too small. To counteract this inappropriate level of depolarisation the muscle could signal to the motoneuron to adjust either the strength of the NMJ[7–9], the size of the dendritic arbor, or a combination of both. Adaptations at the NMJ are well characterised[84,85], such as the increased number of active zones in small, mutant NMJs that can maintain a wild type level of depolarisation in the muscles. Structural homeostasis has also been observed in the *Drosophila* larval central nervous system, although not in response to a retrograde signal. Motoneurons appear to have a preferred level of depolarisation, and when perturbed, will adapt in such a way as to return to this level. Tripodi et al (2008) showed that abolishing neurotransmitter release from the interneurons lead to an extension of the aCC motoneuron dendritic arbor and an increase in complexity. On the other hand, increasing the density of synapses with presynaptic interneurons leads to a retraction of the arbor. The results of this thesis suggest that a localised structural homeostasis may be initiated by a muscle derived retrograde signal. In other words, the muscle could re-set the motoneuron's preferred level of depolarisation if it does not cause an appropriate postsynaptic level of depolarisation.

Retrograde signalling seems particularly necessary when considering that the *Drosophila* motoneurons scale with body size during larval development via the systemic ecdysone hormone[36]. Signalling on such a global scale is unlikely to result in perfectly sized dendritic arbors. With a retrograde signalling mechanism in place, the motoneuron could adapt to naturally occurring variation in muscle size, thus fine tuning the locomotor output.

An assumption in this thesis is that a motoneuron with a larger dendritic tree receives a greater number of synapses that result in an increased number of action potentials and prolonged activity bursts. From work done with the *Drosophila* larval motor system (L.Couton, pers. comm.; Zwart et al. , 2013), the rat superior cervical ganglion (SCG), and ciliary ganglion, most studies have confirmed that this is a fair assumption[1,36,59,113,114,138,139]. For example, Purves and Litchman (1985) showed that the number of axons converging onto the ganglionic cells within the SCG of five small, related

animals correlated with dendritic complexity[140]. While a longer arbor likely means more synaptic connections, it would be interesting to use a presynaptic marker to confirm this. Electrophysiological experiments have recently demonstrated that a larger synaptic drive correlated with larger dendritic arbors (Zwart et al, 2013). To confirm this with the particular genotypes and manipulation I used in this study would have been good to do, but sadly these were both outside the timeframe of this project.

4.3 Contralateral terminal arbor

From my reconstructions I have also been able to measure how the terminal arbor, the total length of terminal tip segments, changes with muscle size. Like the core arbor, my results show a positive correlation between contralateral terminal arbor length and DA1 muscle area when both are normalised to animal size. Terminal branches are motile and have not been stabilised, making it very difficult to infer very much about their dynamics without live imaging. The reconstructions only provide a snap shot of events at a particular developmental stage. While reconstructions do not give any qualitative information regarding terminal arbor dynamics, it does suggest that a correlated change has occurred.

4.4 A localised response?

The results of this thesis suggest that muscle size does have an effect on dendrite morphology, however they also raise new questions. Principally, why is the contralateral, and not the ipislateral arbor affected more strongly? One hypothesis is that the changes in the ipsilateral arbor are more subtle and would require a larger sample size to detect statistically. Support for this hypothesis comes from the significant, positive correlation between the normalised ipsilateral and contralateral core arbor lengths. Alternatively, the results from the contralateral arbor could suggest that the two dendritic arbors respond very differently to the same retrograde signal. This could be analogous to how different compartments of a neuron respond to the same external signalling molecule[102]. For example, the asymmetrical distribution of guanylate cyclase in the pyramidal neurons

of the mammalian cortex determines whether the *semaphorin 3A* external signal acts as a chemoattractant or a chemorepellent. Distribution of such a regulatory protein could make the contralateral arbor more susceptible to dendritic remodelling in response to retrograde signalling.

4.5 What makes a larger arbor?

Having found that the size of the contralateral arbor is significantly affected by the DA1 area, following normalisation, I was interested to establish whether dendritic growth was due to the addition or scaling of branches. With the exception of the terminal branches, previous studies suggest that branch length is relatively constant, and that dendritic growth occurs through the addition of branches[36]. As expected, core branch length in both ipsilateral and contralateral arbors was stable at approximately 2µm, with differences in core arbor lengths determined by variations in branch number.

The ipsilateral arbor, which is seemingly unaffected by a disproportionate target muscle, also revealed some interesting features in the terminal branches. Larger ipsilateral core arbors support a greater terminal arbor, however the average length of a terminal branch decreases with increasing core arbor length. The results of this thesis show that the morphology of the ipsilateral arbor seems not to be affected by retrograde signalling, suggesting that changes in terminal segment length could be an intrinsic characteristic of growth common to all motoneurons. This is consistent with studies demonstrating that the growth rate and degree of synaptic modification decreases as the total size of the dendritic arbor inceases[141].

4.6 Shape and distribution of the dendritic arbor

Sholl analsysis is a method of quantifying the distribution of branch points and branch lengths at consecutive distances from the motoneuron's primary neurite. In accordance with previous studies, there is a bell-shaped distribution of branch points and branch length in the ipsilateral arbor[142,143]. Sholl analysis from the contralateral arbor has a very different shape due to the lower density of branches and different definition of the

primary neurite. Like the ipsilateral arbor, there is not an obvious difference between genotypes in the contralateral arbor.

4.7 Locomotor behaviour

To make sure that the genetic background was not having a global effect on the activity of motor networks, it was necessary to measure the locomotion of larvae from each genotype. This type of control is particularly important when using the RN2 promoter, as the *Gal4* and *LexA* yeast transcription factors are occasionally expressed in the descending and ascending interneurons. By observing that there was no difference in larval crawling between genotypes, it was possible to infer that the changes observed in the MN were due to the muscle size manipulations rather than unforeseen systemic effects. This control also confirmed that DA1 muscle manipulations do not restrict larval locomotion.

4.8 Retrograde signal identity

Unlike the NMJ, *glass bottom boat* (*gbb*) and its receptor, *wishful thinking* (*wit*), appear not to influence dendritic outgrowth in the *Drosophila* larval motoneurons (Zwart, unpublished). While it is an understandable candidate, the expression of a dominant negative *wit* receptor does not induce a mutant phenotype in the aCC motoneuron dendritic arbor. However, there is currently some evidence suggesting that the activins, also members of the bone morphogenetic proteins (BMP), may act as a dendrite-organising retrograde signal. The activins *Dawdle* and *Maverick* are known to act at the neuromuscular junction where they appear to be secreted by NMJ-associated glia cells and act genetically upstream of *gbb* signalling[4,5]. Evidence that they act as retrograde signals comes through expressing dominant negative versions of their receptors, *punt* and *baboon*, in the larval aCC motoneuron. In both cases there are severe reductions in dendritic arbor, however it is not known whether this is a direct or indirect effect, as the NMJ also displayed a mutant phenotype (Zwart, unpublished). An alternative means of determining whether activins determine dendritic morphology is to express a

constitutively active receptor. This was something I tested, but I did not manage to image sufficient motoneurons due to time limitations. Future experiments should definitely establish the effect of the constitutively active *baboon* receptor.

4.9 Presynaptic propagation of retrograde signals

As well as identifying the trans-synaptic signal, establishing the internal signalling mechanism responsible for dendritic modification is important. Tripodi et al (2008) found that the dendritic overgrowth observed when presynaptic neurotransmission was prevented was abolished with the expression of constitutively active *Protein Kinase A* (*PKA*)[113]. *PKA* appears to be a negative regulator of the homeostatic dendritic overgrowth. In light of the results from this project, it would be interesting to investigate whether a decrease in *PKA* activity is involved with the dendritic overgrowth observed in contralateral core arbor. This could reveal whether there is a common or parallel pathways involved in structural homeostasis.

Another interesting question is how the retrograde signal reaches the dendritic arbor. Changes in distant neuronal structures, such as the dendrites, are often due to changes in gene expression. The retrograde signal must therefore travel a considerable distance from the NMJ to the nucleus. Three common mechanisms exist for propagating retrograde signals: cytoskeleton-based axonal transport, regenerative waves of cytosolic secondary messengers, or the passive diffusion of secondary messengers[65].

As members of the *TGF-β* family, the candidate retrograde signal, *activins,* would reach the nucleus by a mechanism very similar to the *gbb* signal[4]. Upon binding the receptor, the activated ligand-receptor complex is endocytosed and transported along the cytoskeleton in association with various motor proteins. Application of colchicine in the rodent *SCG*, which disrupts microtubule polymerisation, produces a phenotype similar to that observed in axotomised ganglion neurons, suggesting that the ligand and activated receptor reaches the nucleus in association with the cytoskeleton[77,144]. This retrograde signal has since been shown to be *NGF,* which is internalised and transported with the *Trk* neurotrophin receptors[145–147]. Due to the positive-end-distal orientation of the

microtubule subunits in the *Drosophila* larval axon, in this model organisms nuclear-bound vesicles are thought to be associated with dynein motor proteins[9].

Alternatively, retrograde signals can reach the nucleus via secondary messengers. These are particularly important for diffusible retrograde signals with short half-lives, such as carbon and nitrogen monoxide (CO and NO)[65]. Secondary messengers are equally necessary for transmembrane proteins that bind between the pre and post-synaptic membranes. These proteins are believed to transmit signals between the cells through structural modification, and cannot be readily endocytosed[65,148]. Common secondary messengers include calcium, cAMP, cGMP and inositol triphosphate (InsP). Due to their small size many of these molecules can diffuse passively over short distances, however the length of many axons is too great for diffusion alone. Calcium is an example of a secondary messenger that signals via regenerative waves. This is particularly obvious during fertilisation[149], in which a calcium wave in initiated at the site of sperm entry, but is also common in neurons[150]. The axonal endoplasmic reticulum forms membranous network along which a regenerative wave could travel by calcium-induced-calcium-release. Altering the local protein composition of the endoplasmic reticulum can change Ca^{2+} homeostasis, influencing protein synthesis throughout the cell. Also, axonal calcium release seems to be involved in coordinating neuronal degeneration in many pathological conditions[151], suggesting that the endoplasmic reticulum may also serve as a pathway along which retrograde signals or secondary messengers could propagate[152,153].

Bibliography

1. Voyvodic, J. T. Peripheral target regulation of dendritic geometry in the rat superior cervical ganglion. *J. Neurosci.* **9,** 1997–2010 (1989).

2. Yawo, H. Changes in the dendritic geometry of mouse superior cervical ganglion cells following postganglionic axotomy. *J. Neurosci.* **7,** 3703–3711 (1987).

3. Purves, D., Snider, W. & Voyvodic, J. T. Trophic regulation of nerve cell morphology and innervation in the autonomic nervous system. *Nature* **336,** 123–128 (1988).

4. Fuentes-Medel, Y. *et al.* Integration of a Retrograde Signal during Synapse Formation by Glia-Secreted TGF-β Ligand. *Curr. Biol.* **22,** 1831–1838 (2012).

5. Ellis, J. E., Parker, L., Cho, J. & Arora, K. Activin signaling functions upstream of Gbb to regulate synaptic growth at the Drosophila neuromuscular junction. *Dev. Biol.* **342,** 121–133 (2010).

6. Tsai, P.-I. *et al.* Activity-dependent retrograde laminin A signaling regulates synapse growth at Drosophila neuromuscular junctions. *Proc. Natl. Acad. Sci. U. S. A.* **109,** 17699–704 (2012).

7. Aberle, H. *et al.* wishful thinking encodes a BMP type II receptor that regulates synaptic growth in Drosophila. *Neuron* **33,** 545–558 (2002).

8. Marqués, G. *et al.* The Drosophila BMP type II receptor Wishful Thinking regulates neuromuscular synapse morphology and function. *Neuron* **33,** 529–543 (2002).

9. McCabe, B. D. *et al.* The BMP homolog Gbb provides a retrograde signal that regulates synaptic growth at the Drosophila neuromuscular junction. *Neuron* **39,** 241–254 (2003).

10. Bayat, V., Jaiswal, M. & Bellen, H. J. The BMP signaling pathway at the Drosophila neuromuscular junction and its links to neurodegenerative diseases. *Curr. Opin. Neurobiol.* **21,** 182–188 (2011).

11. Ball, R. W. *et al.* Retrograde BMP signaling controls synaptic growth at the NMJ by regulating trio expression in motor neurons. *Neuron* **66,** 536–549 (2010).

12. Penney, J. *et al.* TOR Is Required for the Retrograde Regulation of Synaptic Homeostasis at the Drosophila Neuromuscular Junction. *Neuron* **74,** 166–178 (2012).

13. Iremonger, K. J., Wamsteeker Cusulin, J. I. & Bains, J. S. Changing the tune: Plasticity and adaptation of retrograde signals. *Trends Neurosci.* **36,** 471–479 (2013).

14. Greenspan, R. J. *Fly pushing: The theory and Practice of Drosophila Genetics*. 192 (Cold Spring Harbor Laboratory Press, 2004).

15. Kohsaka, H., Okusawa, S., Itakura, Y., Fushiki, A. & Nose, A. Development of larval motor circuits in Drosophila. *Dev. Growth Differ.* **54,** 408–19 (2012).

16. Landgraf, M. & Thor, S. Development of Drosophila motoneurons: Specification and morphology. *Semin. Cell Dev. Biol.* **17,** 3–11 (2006).

17. John Roote* and Andreas Prokop. How to design a genetic mating scheme: a basic training package for Drosophila genetics. 1–12

18. Roote, J. & Prokop, A. How to design a genetic mating scheme: a basic training package for Drosophila genetics. *G3 (Bethesda).* **3,** 353–8 (2013).

19. Del Valle Rodríguez, A., Didiano, D. & Desplan, C. Power tools for gene expression and clonal analysis in Drosophila. *Nat. Methods* **9,** 47–55 (2011).

20. Risse, B. *et al.* FIM, a Novel FTIR-Based Imaging Method for High Throughput Locomotion Analysis. *PLoS One* **8,** (2013).

21. Bate, M. The embryonic development of larval muscles in Drosophila. *Development* **110,** 791–804 (1990).

22. Kohsaka, H., Okusawa, S., Itakura, Y., Fushiki, A. & Nose, A. Development of larval motor circuits in Drosophila. *Dev. Growth Differ.* **54,** 408–419 (2012).

23. Berrigan, D. & Pepin, D. J. How maggots move: Allometry and kinematics of crawling in larval Diptera. *J. Insect Physiol.* **41,** 329–337 (1995).

24. Suster, M. L. & Bate, M. Embryonic assembly of a central pattern generator without sensory input. *Nature* **416,** 174–178 (2002).

25. Fox, L. E., Soll, D. R. & Wu, C.-F. Coordination and modulation of locomotion pattern generators in Drosophila larvae: effects of altered biogenic amine levels by the tyramine beta hydroxlyase mutation. *J. Neurosci.* **26,** 1486–1498 (2006).

26. Kim, M. D., Wen, Y. & Jan, Y. N. Patterning and organization of motor neuron dendrites in the Drosophila larva. *Dev. Biol.* **336,** 213–221 (2009).

27. Landgraf, M., Bossing, T., Technau, G. M. & Bate, M. The origin, location, and projections of the embryonic abdominal motorneurons of Drosophila. *J. Neurosci.* **17,** 9642–9655 (1997).

28. Baines, R. A., Seugnet, L., Thompson, A., Salvaterra, P. M. & Bate, M. Regulation of synaptic connectivity: levels of Fasciclin II influence synaptic growth in the Drosophila CNS. *J. Neurosci.* **22,** 6587–6595 (2002).

29. Baines, R. A. Development of Motoneuron Electrical Properties and Motor Output. *Int. Rev. Neurobiol.* **75,** 91–103 (2006).

30. Rohrbough, J. & Broadie, K. Electrophysiological analysis of synaptic transmission in central neurons of Drosophila larvae. *J. Neurophysiol.* **88,** 847–860 (2002).

31. Marder, E. & Bucher, D. Central pattern generators and the control of rhythmic movements. *Curr. Biol.* **11,** (2001).

32. Grillner, S. The motor infrastructure: from ion channels to neuronal networks. *Nat. Rev. Neurosci.* **4,** 573–586 (2003).

33. MacKay-Lyons, M. Central pattern generation of locomotion: a review of the evidence. *Phys. Ther.* **82,** 69–83 (2002).

34. Landgraf, M., Roy, S., Prokop, A., VijayRaghavan, K. & Bate, M. even-skipped determines the dorsal growth of motor axons in Drosophila. *Neuron* **22,** 43–52 (1999).

35. Hoang, B. & Chiba, A. Single-cell analysis of Drosophila larval neuromuscular synapses. *Dev. Biol.* **229,** 55–70 (2001).

36. Zwart, M. F., Randlett, O., Evers, J. F. & Landgraf, M. Dendritic growth gated by a steroid hormone receptor underlies increases in activity in the developing Drosophila locomotor system. *Proc. Natl. Acad. Sci. U. S. A.* **110,** E3878–87 (2013).

37. Zito, K., Parnas, D., Fetter, R. D., Isacoff, E. Y. & Goodman, C. S. Watching a synapse grow: Noninvasive confocal imaging of synaptic growth in Drosophila. *Neuron* **22,** 719–729 (1999).

38. Schuster, C. M., Davis, G. W., Fetter, R. D. & Goodman, C. S. Genetic dissection of structural and functional components of synaptic plasticity. I. Fasciclin II controls synaptic stabilization and growth. *Neuron* **17,** 641–654 (1996).

39. Koles, K. & Budnik, V. Wnt signaling in neuromuscular junction development. *Cold Spring Harb. Perspect. Biol.* **4,** 1–22 (2012).

40. Korkut, C. & Budnik, V. WNTs tune up the neuromuscular junction. *Nat. Rev. Neurosci.* **10,** 627–634 (2009).

41. Packard, M. *et al.* The Drosophila Wnt, wingless, provides an essential signal for pre- and postsynaptic differentiation. *Cell* **111,** 319–330 (2002).

42. Ataman, B. *et al.* Rapid Activity-Dependent Modifications in Synaptic Structure and Function Require Bidirectional Wnt Signaling. *Neuron* **57,** 705–718 (2008).

43. Zarnescu, D. C. & Zinsmaier, K. E. Ferrying Wingless across the Synaptic Cleft. *Cell* **139,** 229–231 (2009).

44. Mathew, D. *et al.* Wingless signaling at synapses is through cleavage and nuclear import of receptor DFrizzled2. *Science* **310,** 1344–1347 (2005).

45. Miech, C., Pauer, H.-U., He, X. & Schwarz, T. L. Presynaptic local signaling by a canonical wingless pathway regulates development of the Drosophila neuromuscular junction. *J. Neurosci.* **28,** 10875–10884 (2008).

46. Liebl, F. L. W. *et al.* Derailed regulates development of the Drosophila neuromuscular junction. *Dev. Neurobiol.* **68,** 152–165 (2008).

47. Goodman, R. M. *et al.* Sprinter: a novel transmembrane protein required for Wg secretion and signaling. *Development* **133,** 4901–4911 (2006).

48. Rubin, E. Development of the rat superior cervical ganglion: ganglion cell maturation. *J. Neurosci.* **5,** 673–684 (1985).

49. Gao, F. B., Brenman, J. E., Jan, L. Y. & Jan, Y. N. Genes regulating dendritic outgrowth, branching, and routing in Drosophila. *Genes Dev.* **13,** 2549–2561 (1999).

50. Dailey, M. E. & Smith, S. J. The dynamics of dendritic structure in developing hippocampal slices. *J. Neurosci.* **16,** 2983–2994 (1996).

51. Bhatt, D. H., Zhang, S. & Gan, W.-B. Dendritic spine dynamics. *Annu. Rev. Physiol.* **71,** 261–282 (2009).

52. Niell, C. M. & Smith, S. J. Live optical imaging of nervous system development. *Annu. Rev. Physiol.* **66,** 771–798 (2004).

53. Scott, E. K. & Luo, L. How do dendrites take their shape? *Nat. Neurosci.* **4,** 359–365 (2001).

54. Purves D, H. R. Changes in the dendritic branching of adult mammalian neurones revealed by repeated imaging in situ. *Nature* **315,** 404–6 (1985).

55. Niell, C. M., Meyer, M. P. & Smith, S. J. In vivo imaging of synapse formation on a growing dendritic arbor. *Nat. Neurosci.* **7,** 254–260 (2004).

56. Kossel, A. H., Williams, C. V, Schweizer, M. & Kater, S. B. Afferent innervation influences the development of dendritic branches and spines via both activity-dependent and non-activity-dependent mechanisms. *J. Neurosci.* **17,** 6314–6324 (1997).

57. Lohmann, C., Myhr, K. L. & Wong, R. O. L. Transmitter-evoked local calcium release stabilizes developing dendrites. *Nature* **418,** 177–181 (2002).

58. Lohmann, C. & Wong, R. O. L. Regulation of dendritic growth and plasticity by local and global calcium dynamics. *Cell Calcium* **37,** 403–409 (2005).

59. Tavosanis, G. Dendritic structural plasticity. *Dev. Neurobiol.* **72,** 73–86 (2012).

60. Corty, M. M., Matthews, B. J. & Grueber, W. B. Molecules and mechanisms of dendrite development in Drosophila. *Development* **136,** 1049–1061 (2009).

61. Kaech, S., Parmar, H., Roelandse, M., Bornmann, C. & Matus, A. Cytoskeletal microdifferentiation: a mechanism for organizing morphological plasticity in dendrites. *Proc. Natl. Acad. Sci. U. S. A.* **98,** 7086–7092 (2001).

62. Rolls, M. M. Neuronal polarity in Drosophila: Sorting out axons and dendrites. *Dev. Neurobiol.* **71,** 419–429 (2011).

63. Fujioka, M. *et al.* Embryonic even skipped-dependent muscle and heart cell fates are required for normal adult activity, heart function, and lifespan. *Circ. Res.* **97,** 1108–1114 (2005).

64. Satoh, D., Sato, D., Tsuyama, T., Saito, M., Ohkura, H., Rolls, M.M., Ishikawa, F., Uemura, T. Spatial control of branching within dendritic arbors by dynein-dependent transport of Rab5-endosomes. *Nat. Cell Biol.* **10,** 1164–1171 (2008).

65. Fitzsimonds, R. M. & Poo, M. M. Retrograde signaling in the development and modification of synapses. *Physiol. Rev.* **78,** 143–70 (1998).

66. Harrington, A. W. & Ginty, D. D. Long-distance retrograde neurotrophic factor signalling in neurons. *Nat. Rev. Neurosci.* **14,** 177–87 (2013).

67. Cattaneo, A. Immunosympathectomy as the first phenotypic knockout with antibodies. *Proc. Natl. Acad. Sci. U. S. A.* **110,** 4877–4885 (2013).

68. Lewin, G. R. & Barde, Y. A. Physiology of the neurotrophins. *Annu. Rev. Neurosci.* **19,** 289–317 (1996).

69. Baines, R. A. Synaptic strengthening mediated by bone morphogenetic protein-dependent retrograde signaling in the Drosophila CNS. *J. Neurosci.* **24,** 6904–6911 (2004).

70. Salinas, P. C. Retrograde signalling at the synapse: a role for Wnt proteins. *Biochem. Soc. Trans.* **33,** 1295–1298 (2005).

71. Wang T, Hauswirth AG, Tong A, Dickman DK, D. G. Endostatin is a trans-synaptic signal for homeostatic synaptic plasticity. *Neuron* **83,** 616–29 (2014).

72. Schuman, E. M. & Madison, D. V. Nitric oxide and synaptic function. *Annu. Rev. Neurosci.* **17,** 153–183 (1994).

73. Gottmann, K. Transsynaptic modulation of the synaptic vesicle cycle by cell-adhesion molecules. *J. Neurosci. Res.* **86,** 223–232 (2008).

74. Wu, H., Xiong, W. C. & Mei, L. To build a synapse: signaling pathways in neuromuscular junction assembly. *Development* **137,** 1017–33 (2010).

75. Voyvodic, T. Peripheral Target Regulation Superior Cervical Ganglion of Dendritic Geometry in the Rat. (2010).

76. Purves, D. Functional and structural changes in mammalian sympathetic neurones following interruption of their axons. *J. Physiol.* **252,** 429–463 (1975).

77. Pilar, G. & Landmesser, L. Axotomy mimicked by localized colchicine application. *Science* **177,** 1116–1118 (1972).

78. Watson WE. Cellular responses to axotomy and to related procedures. *Br Med Bull.* **30,** 112–5 (1974).

79. Sumner BE, W. W. Retraction and expansion of the dendritic tree of motor neurones of adult rats induced in vivo. *Nature* **233,** 273–5 (1971).

80. Snider, W. D. Nerve growth factor enhances dendritic arborization of sympathetic ganglion cells in developing mammals. *J Neurosci* **8,** 2628–2634 (1988).

81. Rose, P. K. & Odlozinski, M. Expansion of the dendritic tree of motoneurons innervating neck muscles of the adult cat after permanent axotomy. *J. Comp. Neurol.* **390,** 392–411 (1998).

82. Johnson, L. A., Kristan, W. B., Jellies, J. & French, K. A. Disruption of peripheral target contact influences the development of identified central dendritic branches in a leech motor neuron in vivo. *J. Neurobiol.* **43,** 365–378 (2000).

83. Stewart, B. A., Schuster, C. M., Goodman, C. S. & Atwood, H. L. Homeostasis of synaptic transmission in Drosophila with genetically altered nerve terminal morphology. *J. Neurosci.* **16,** 3877–3886 (1996).

84. Paradis, S., Sweeney, S. T. & Davis, G. W. Homeostatic control of presynaptic release is triggered by postsynaptic membrane depolarization. *Neuron* **30,** 737–749 (2001).

85. Davis, G. W. Homeostatic control of neural activity: from phenomenology to molecular design. *Annu. Rev. Neurosci.* **29,** 307–323 (2006).

86. Krishnaswamy, A. & Cooper, E. An Activity-Dependent Retrograde Signal Induces the Expression of the High-Affinity Choline Transporter in Cholinergic Neurons. *Neuron* **61,** 272–286 (2009).

87. Haghighi, a P. *et al.* Retrograde control of synaptic transmission by postsynaptic CaMKII at the Drosophila neuromuscular junction. *Neuron* **39,** 255–267 (2003).

88. Baines, R. a. Synaptic strengthening mediated by bone morphogenetic protein-dependent retrograde signaling in the Drosophila CNS. *J. Neurosci.* **24,** 6904–6911 (2004).

89. Bartlett, W. P. & Banker, G. A. An electron microscopic study of the development of axons and dendrites by hippocampal neurons in culture. I. Cells which develop without intercellular contacts. *J. Neurosci.* **4,** 1944–1953 (1984).

90. Bray, D. Branching patterns of individual sympathetic neurons in culture. *J. Cell Biol.* **56,** 702–712 (1973).

91. Parrish, J. Z., Emoto, K., Kim, M. D. & Jan, Y. N. Mechanisms that regulate establishment, maintenance, and remodeling of dendritic fields. *Annu. Rev. Neurosci.* **30,** 399–423 (2007).

92. Jan, Y. N. & Jan, L. Y. The Control of Dendrite Development. *Neuron* **40,** 229–242 (2003).

93. Goldberg, J. L. Intrinsic neuronal regulation of axon and dendrite growth. *Curr. Opin. Neurobiol.* **14,** 551–557 (2004).

94. Moore, A. W., Jan, L. Y. & Jan, Y. N. hamlet, a binary genetic switch between single- and multiple- dendrite neuron morphology. *Science* **297,** 1355–1358 (2002).

95. Li, W., Wang, F., Menut, L. & Gao, F. B. BTB/POZ-zinc finger protein abrupt suppresses dendritic branching in a neuronal subtype-specific and dosage-dependent manner. *Neuron* **43,** 823–834 (2004).

96. Sugimura, K., Satoh, D., Estes, P., Crews, S. & Uemura, T. Development of morphological diversity of dendrites in Drosophila by the BTB-zinc finger protein abrupt. *Neuron* **43,** 809–822 (2004).

97. Parrish, J. Z., Kim, M. D., Jan, L. Y. & Jan, Y. N. Genome-wide analyses identify transcription factors required for proper morphogenesis of Drosophila sensory neuron dendrites. *Genes Dev.* **20,** 820–835 (2006).

98. Li, Z., Van Aelst, L. & Cline, H. T. Rho GTPases regulate distinct aspects of dendritic arbor growth in Xenopus central neurons in vivo. *Nat. Neurosci.* **3,** 217–225 (2000).

99. Luo, L. Actin cytoskeleton regulation in neuronal morphogenesis and structural plasticity. *Annu. Rev. Cell Dev. Biol.* **18,** 601–635 (2002).

100. Prokop, A., Uhler, J., Roote, J. & Bate, M. The kakapo mutation affects terminal arborization and central dendritic sprouting of Drosophila motorneurons. *J. Cell Biol.* **143,** 1283–1294 (1998).

101. Furrer, M.-P., Vasenkova, I., Kamiyama, D., Rosado, Y. & Chiba, A. Slit and Robo control the development of dendrites in Drosophila CNS. *Development* **134,** 3795–3804 (2007).

102. Polleux, F., Morrow, T. & Ghosh, A. Semaphorin 3A is a chemoattractant for cortical apical dendrites. *Nature* **404,** 567–573 (2000).

103. Kim, S. & Chiba, A. Dendritic guidance. *Trends Neurosci.* **27,** 194–202 (2004).

104. Furrer, M.-P., Kim, S., Wolf, B. & Chiba, A. Robo and Frazzled/DCC mediate dendritic guidance at the CNS midline. *Nat. Neurosci.* **6,** 223–230 (2003).

105. Rosso, S. B., Sussman, D., Wynshaw-Boris, A. & Salinas, P. C. Wnt signaling through Dishevelled, Rac and JNK regulates dendritic development. *Nat. Neurosci.* **8,** 34–42 (2005).

106. Ruchhoeft, M. L., Ohnuma, S., McNeill, L., Holt, C. E. & Harris, W. A. The neuronal architecture of Xenopus retinal ganglion cells is sculpted by rho-family GTPases in vivo. *J. Neurosci.* **19,** 8454–8463 (1999).

107. Lee, T., Winter, C., Marticke, S. S., Lee, A. & Luo, L. Essential roles of Drosophila RhoA in the regulation of neuroblast proliferation and dendritic but not axonal morphogenesis. *Neuron* **25,** 307–316 (2000).

108. Volkmar, F. R. & Greenough, W. T. Rearing complexity affects branching of dendrites in the visual cortex of the rat. *Science* **176,** 1445–1447 (1972).

109. Ralph L. Holloway Jr. Dendritic branching: some preliminary results of training and complexity in rat visual cortex. **3,** 337–352 (1967).

110. Feng, A. S. & Rogowski, B. A. Effects of monaural and binaural occlusion on the morphology of neurons in the medial superior olivary nucleus of the rat. *Brain Res.* **189,** 530–534 (1980).

111. Pasic, T. R., Moore, D. R. & Rubel, E. W. Effect of altered neuronal activity on cell size in the medial nucleus of the trapezoid body and ventral cochlear nucleus of the gerbil. *J. Comp. Neurol.* **348,** 111–20 (1994).

112. Hartwig, C. L., Worrell, J., Levine, R. B., Ramaswami, M. & Sanyal, S. Normal dendrite growth in Drosophila motor neurons requires the AP-1 transcription factor. *Dev. Neurobiol.* **68,** 1225–1242 (2008).

113. Tripodi, M., Evers, J. F., Mauss, A., Bate, M. & Landgraf, M. Structural homeostasis: Compensatory adjustments of dendritic arbor geometry in response to variations of synaptic input. *PLoS Biol.* **6,** 2172–2187 (2008).

114. Purves, D. & Hume, R. I. The relation of postsynaptic geometry to the number of presynaptic axons that innervate autonomic ganglion cells. *J. Neurosci.* **1,** 441–452 (1981).

115. Goodman, C. S. Isogenic grasshoppers: genetic variability in the morphology of identified neurons. *J. Comp. Neurol.* **182,** 681–705 (1978).

116. Landgraf, M., Jeffrey, V., Fujioka, M., Jaynes, J. B. & Bate, M. Embryonic origins of a motor system: Motor dendrites form a myotopic map in Drosophila. *PLoS Biol.* **1,** (2003).

117. Mauss, A., Tripodi, M., Evers, J. F. & Landgraf, M. Midline signalling systems direct the formation of a neural map by dendritic targeting in the Drosophila motor system. *PLoS Biol.* **7,** (2009).

118. Leevers, S. J., Weinkove, D., MacDougall, L. K., Hafen, E. & Waterfield, M. D. The Drosophila phosphoinositide 3-kinase Dp110 promotes cell growth. *EMBO J.* **15,** 6584–94 (1996).

119. Rommel, C. *et al.* Mediation of IGF-1-induced skeletal myotube hypertrophy by PI(3)K/Akt/mTOR and PI(3)K/Akt/GSK3 pathways. *Nat. Cell Biol.* **3,** 1009–1013 (2001).

120. Glass, D. J. Molecular mechanisms modulating muscle mass. **9,** 344–350 (2003).

121. Weiss, a, Herzig, a, Jacobs, H. & Lehner, C. F. Continuous Cyclin E expression inhibits progression through endoreduplication cycles in Drosophila. *Curr. Biol.* **8,** 239–42 (1998).

122. Zielke, N., Edgar, B. a & DePamphilis, M. L. Endoreplication. *Cold Spring Harb. Perspect. Biol.* **5,** a012948 (2013).

123. Fujioka, M. *et al.* Even-skipped, acting as a repressor, regulates axonal projections in Drosophila. *Development* **130,** 5385–5400 (2003).

124. Roy, B. *et al.* Metamorphosis of an identified serotonergic neuron in the Drosophila olfactory system. *Neural Dev.* **2,** 20 (2007).

125. Pfeiffer, B. D. *et al.* Refinement of tools for targeted gene expression in Drosophila. *Genetics* **186,** 735–755 (2010).

126. Pfeiffer, B. D. *et al.* Tools for neuroanatomy and neurogenetics in Drosophila. *Proc. Natl. Acad. Sci. U. S. A.* **105,** 9715–9720 (2008).

127. Leevers, S. J., Weinkove, D., MacDougall, L. K., Hafen, E. & Waterfield, M. D. The Drosophila phosphoinositide 3-kinase Dp110 promotes cell growth. *EMBO J.* **15,** 6584–6594 (1996).

128. Brierley, D. J., Blanc, E., Reddy, O. V., VijayRaghavan, K. & Williams, D. W. Dendritic targeting in the leg neuropil of Drosophila: The role of midline signalling molecules in generating a myotopic map. *PLoS Biol.* **7,** (2009).

129. Schmitt, S., Evers, J. F., Duch, C., Scholz, M. & Obermayer, K. New methods for the computer-assisted 3-D reconstruction of neurons from confocal image stacks. *Neuroimage* **23,** 1283–1298 (2004).

130. Evers, J. F., Schmitt, S., Sibila, M. & Duch, C. Progress in functional neuroanatomy: precise automatic geometric reconstruction of neuronal morphology from confocal image stacks. *J. Neurophysiol.* **93,** 2331–2342 (2005).

131. Sokolowski, M. B. Drosophila: genetics meets behaviour. *Nat. Rev. Genet.* **2,** 879–890 (2001).

132. Han, J. Y. Low-cost multi-touch sensing through frustrated total internal reflection. *Proc. 18th Annu. ACM Symp. User interface Softw. Technol. - UIST '05* 115–118 (2005). doi:10.1145/1095034.1095054

133. Leevers, S. J., Weinkove, D., MacDougall, L. K., Hafen, E. & Waterfield, M. D. The Drosophila phosphoinositide 3-kinase Dp110 promotes cell growth. *EMBO J.* **15,** 6584–6594 (1996).

134. Sigrist, S. J., Reiff, D. F., Thiel, P. R., Steinert, J. R. & Schuster, C. M. Experience-dependent strengthening of Drosophila neuromuscular junctions. *J. Neurosci.* **23,** 6546–6556 (2003).

135. Sokolowski, M. B., Kent, C. & Wong, J. Drosophila larval foraging behaviour: Developmental stages. *Anim. Behav.* **32,** 645–651 (1984).

136. Ghannad-Rezaie, M., Wang, X., Mishra, B., Collins, C. & Chronis, N. Microfluidic chips for in vivo imaging of cellular responses to neural injury in Drosophila larvae. *PLoS One* **7,** (2012).

137. MacDermid, V., Neuber-Hess, M., Short, C. & Rose, P. K. Alterations to neuronal polarity following permanent axotomy: A quantitative analysis of changes to

MAP2a/b and GAP-43 distributions in axotomized motoneurons in the adult cat. *J. Comp. Neurol.* **450,** 318–333 (2002).

138. Purves, D. & Lichtman, J. W. Geometrical differences among homologous neurons in mammals. *Science* **228,** 298–302 (1985).

139. PURVES, R. I. H. & D. Geometry of neonatal neurones and the regulation of synapse elimination. *Nature* **293,** 469 – 471 (1981).

140. Purves, D. & Lichtman, J. W. Geometrical differences among homologous neurons in mammals. *Science* **228,** 298–302 (1985).

141. Wu, G. Y., Zou, D. J., Rajan, I. & Cline, H. Dendritic dynamics in vivo change during neuronal maturation. *J. Neurosci.* **19,** 4472–4483 (1999).

142. Timmerman, C. *et al.* The Drosophila transcription factor Adf-1 (nalyot) regulates dendrite growth by controlling FasII and Staufen expression downstream of CaMKII and neural activity. *J. Neurosci.* **33,** 11916–31 (2013).

143. Mishra, A., Knerr, B., Paixão, S., Kramer, E. R. & Klein, R. The protein dendrite arborization and synapse maturation 1 (Dasm-1) is dispensable for dendrite arborization. *Mol. Cell. Biol.* **28,** 2782–2791 (2008).

144. Purves, D. Functional and structural changes in mammalian sympathetic neurones following colchicine application to post-ganglionic nerves. *J. Physiol.* **259,** 159–175 (1976).

145. Howe, C. L. & Mobley, W. C. Signaling Endosome Hypothesis: A Cellular Mechanism for Long Distance Communication. *J. Neurobiol.* **58,** 207–216 (2004).

146. Von Bartheld, C. S. *et al.* Retrograde transport of neurotrophins from the eye to the brain in chick embryos: roles of the p75NTR and trkB receptors. *J. Neurosci.* **16,** 2995–3008 (1996).

147. DiStefano, P. S. *et al.* The neurotrophins BDNF, NT-3, and NGF display distinct patterns of retrograde axonal transport in peripheral and central neurons. *Neuron* **8,** 983–993 (1992).

148. Lisman, J. E. & Harris, K. M. Quantal analysis and synaptic anatomy - Integrating two views of hippocampal plasticity. *Trends Neurosci.* **16,** 141–147 (1993).

149. Gilkey, J. C., Jaffe, L. F., Ridgway, E. B. & Reynolds, G. T. A free calcium wave traverses the activating egg of the medaka, Oryzias latipes. *J. Cell Biol.* **76,** 448–466 (1978).

150. Gu, X. & Spitzer, N. C. Distinct aspects of neuronal differentiation encoded by frequency of spontaneous Ca2+ transients. *Nature* **375,** 784–787 (1995).

151. Villegas, R. *et al.* Calcium release from intra-axonal endoplasmic reticulum leads to axon degeneration through mitochondrial dysfunction. *J. Neurosci.* **34,** 7179–89 (2014).

152. Berridge, M. J. The endoplasmic reticulum: A multifunctional signaling organelle. *Cell Calcium* **32,** 235–249 (2002).

153. Chiu, V. K. *et al.* Ras signalling on the endoplasmic reticulum and the Golgi. *Nat. Cell Biol.* **4,** 343–350 (2002).